AD-A263 265

COMPOSITE UNIT ACCELERATED LIFE TEST
OF THE HIGH GAIN ARRAY

Contract Number N00014-93-C-2021

January 28, 1992

DTIC
ELECTE
APR 23 1993
S
B

COMPOSITE UNIT ACCELERATED LIFE TEST
OF THE HIGH GAIN ARRAY

Contract Number N00014-93-C-2021

January 28, 1992

Prepared for:

Commanding Officer
Naval Research Laboratory
Underwater Sound Reference Detachment
Attn: Code 5977 (A.C. Tims)

Naval Surface Warfare Center
CARDEROCK DIV.
Attn: Code 1925 (H. Stottmeister)

93 4 22 042

375436 93-08702
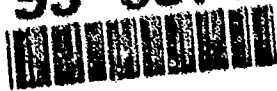
Prepared by:

Texas Research Institute Austin, Inc. (TRI/Austin)
Reliability Engineering Division
A.V. Bray, S.L. Arnett, and S.C. Liberty
9063 Bee Caves Road
Austin, Texas 78733
(512) 263-2101

REPORT DOCUMENTATION PAGE

1. AGENCY USE ONLY (Leave blank)	2. REPORT DATE	3. REPORT TYPE AND DATES COVERED
	8 Jan 1993	Final (Jul-Nov 1992)

4. TITLE AND SUBTITLE
Composite Unit Accelerated Life Test of the High Gain Array

5. FUNDING NUMBERS
C - N00014-93-C-2021
PE - 63504N
TA - S0223
WU - DN 780-137

6. AUTHOR(S)
A.V. Bray, S.L. Arnett, and S.C. Liberty

7. PERFORMING ORGANIZATION NAME(S) AND ADDRESS(ES)
Texas Research Institute Austin, Inc.
9063 Bee Caves Road
Austin, TX 78733

8. PERFORMING ORGANIZATION REPORT NUMBER
A7301-104:AVB-D141.2.1

9. SPONSORING/MONITORING AGENCY NAME(S) AND ADDRESS(ES)
Naval Research Laboratory
Underwater Sound Reference Detachment
P.O. Box 568337
Orlando, FL 32856-8337

10. SPONSORING/MONITORING AGENCY REPORT NUMBER

11. SUPPLEMENTARY NOTES
This work was sponsored by the Carderock Division (Code 1925, H. Stottmeister), Naval Surface Warfare Center, Bethesda, MD 20084-5000.

12a. DISTRIBUTION/AVAILABILITY STATEMENT

Approved for public release; distribution unlimited.

12b. DISTRIBUTION CODE

13. ABSTRACT (Maximum 200 words)
This report documents the composite unit life testing (CUALT) of a 20-element hydrophone array. The array was subjected to a CUALT which simulated five years of service life. After CUALT was completed, an autopsy was performed on the array to determine failure modes and mechanisms. This report also documents array design, mission profile, CUALT schedule and measurement data, autopsy results, and failure analysis.

14. SUBJECT TERMS
Accelerated life testing
Hydrophone array
Hydrophone reliability

15. NUMBER OF PAGES
44

16. PRICE CODE

17. SECURITY CLASSIFICATION OF REPORT	18. SECURITY CLASSIFICATION OF THIS PAGE	19. SECURITY CLASSIFICATION OF ABSTRACT	20. LIMITATION OF ABSTRACT
UNCLASSIFIED	UNCLASSIFIED	UNCLASSIFIED	UL

TABLE OF CONTENTS

DTIC QUALITY INSPECTED 4

LIST OF TABLES

LIST OF FIGURES

1.0 INTRODUCTION

A High Gain Array (HGA) prototype stave was received at the NRL composite unit accelerated life test (CUALT) facility in the 2nd Quarter FY92. A five equivalent year (EY) ALT was concluded in November 1992 and the stave was then sent to TRI/Austin for post-ALT autopsy. This TRI/Austin report details test and autopsy results for the HGA prototype stave.

1.1 Test Article Description

The prototype HGA stave consists of 20 passive hydrophone elements in a line array as shown in Figure 1. Each hydrophone has two ceramic elements in series with an aluminum spool to provide air backing and axial passage of the stave cable. Figure 2 is a schematic diagram of the hydrophone provided as part of the documentation for the ALT stave.

Each hydrophone includes a printed circuit board (PCB) which is encapsulated in a separate molding stage. The PCB is U-shaped to fit around the cable. The entire element is potted and connected to a stave cable consisting of 30 bundled conductors, an outer braided binder, and an inner strength member of Kevlar® with a braided binder. Twenty-four of the conductors are coaxial with a center, signal conductor of 28 AWG tin-plated copper and a 38 AWG tin-plated copper shield. Six of the wires are configured with a single, seven-stranded copper conductor of 24 AWG. The stave cable bundle, and thus the center of the hydrophone elements, is free flooded. The stave cable is terminated in a 37-pin connector with two mechanical terminations of the braided binders and Kevlar® strength members.
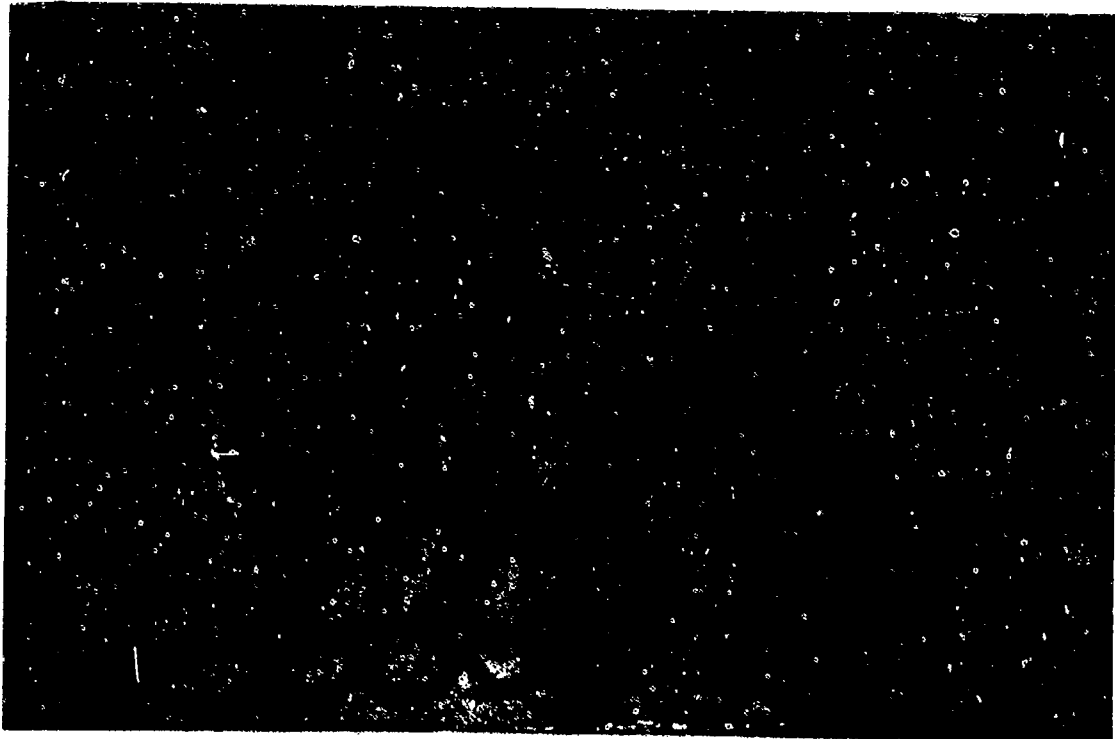
Figure 1. HGA Stave
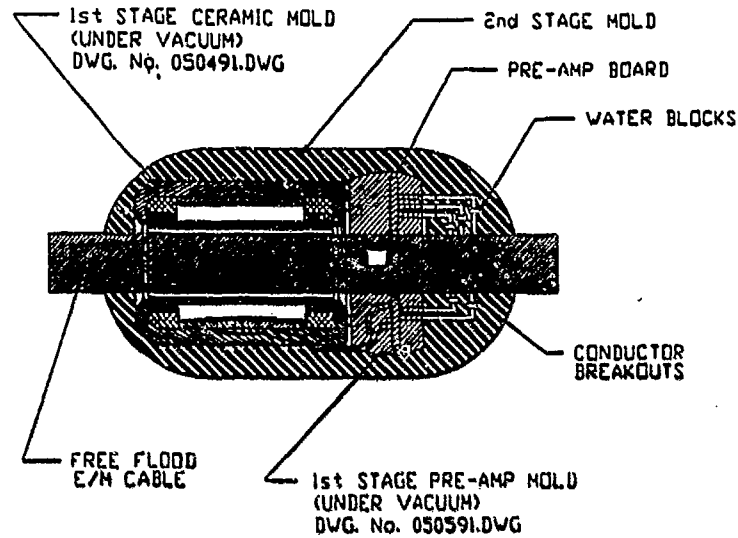
DWG. No. 050391.DWG

Figure 2. Schematic Diagram of a HGA Hydrophone

1.2 Mission Profile, ALT Schedule and Measurements

Appendix A contains the mission profile provided by Naval Surface Warfare Center, CARDEROCK DIV. for the HGA stave. Table 1 summarizes the primary mission and corresponding ALT exposures. All accelerated times were computed using a classic Arrhenius relation and a 13.3 kcal/mole activation energy. This value corresponds to a nominal activation energy for the diffusion of water into polymeric materials. A discussion of the means by which accelerated test times are determined is included as Appendix B.

Table 1. Primary Mission Profile for One Year and Corresponding ALT Exposures

MISSION PROFILE		CUALT EXPOSURE
DEPTH:	400 – 1600 ft.	HYDROSTATIC PRESSURE: 750 psig (NO ACCELERATION) 124 hrs.
AIR EXPOSURE:	1/2 YEAR (ON DECK)	ENVIRONMENTAL CHAMBER: TEMP.: 70 °C UV: 607 μW/cm^2 OZONE: 0.2 ppm 181 hrs.
WET EXPOSURE:	1/2 YEAR FLORIDA LATITUDE	HOT SOAK: TEMP.: 70°C SALT WATER 150 hrs.
		TOTAL HOURS: 455 hrs.

The term of the test was five equivalent years, where an equivalent year is defined as that amount of stress exposure corresponding to a year of service, and is summarized for the HGA in Table 1. Measurements of hydrophone gain were made using a HP-4192A impedance analyzer and associated PC based control/collection system shown schematically in Figure 3. These measurements were made at the end of each EY.
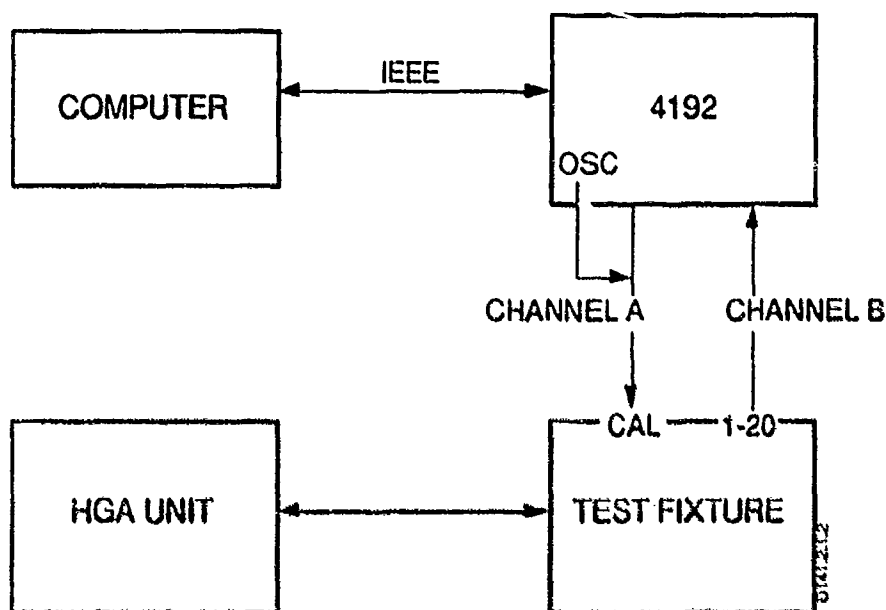
Figure 3. HP-4192A Impedance Analyzer and PC-Based Control/Collection System

In addition, insulation resistance (IR) and surface hardness measurements were made each EY. The IR data were collected with a standard laboratory ohmmeter as opposed to a high voltage IR measuring device (megohmmeters) to prevent damage to the hydrophones from overvoltage in testing. The surface hardness measurements were made at the same location throughout the test using a Shore A hardness tester.

There were two procedures employed during the ALT which impacted the data. The first involved dividing the hydrophone gain measurements into two frequency ranges, 0.1 to 1.0 kHz and 1.0 kHz to 100 kHz. These measurements were made serially such that all the low frequency data were collected first, followed by the high frequency data. The result was that many elements had low frequency data collected on a different day than high band data, causing a shift in the data at 1 kHz that was an artifact of the measurement procedure rather than a hydrophone response problem. These data were corrected in final processing to provide a continuous response curve, and where corrections were made the data are annotated.

In the original ALT schedule the response measurements were routinely made after the hydrostatic pressure cycle. It was noticed during EY 4 that the hydrophones were responding in an odd manner after the pressure test, and in EY 5 the order of exposures was changed such that response measurements were made after an elevated temperature air exposure. The result was that the hydrophone response for elements which had been marginal through EY 4 actually improved in EY 5. This is a clear indication that many of the elements were experiencing drying in the hot air exposure and had some amount of water ingression from the wet pressurized exposures. This effect is not uncommon and a change in exposure order of this type often highlights an otherwise subtle watertight integrity problem.

2.0   ALT RESULTS

2.1   Hydrophone Gain Data

Figure 4 is an example set of hydrophone gain response curves for element H2 of the HGA prototype stave. Note that there is little or no variation from one EY to another for this element. Figure 5 shows the same data for element H10, whose response appears to be erratic for the EY 4 measurement period. The roll-off of EY 4 changed dramatically from the baseline data of EY 0 but was back to normal in EY 5 – an indication that the hot air exposure prior to the EY 5 measurement removed from the unit the moisture that had evidently been a problem in EY 4. The response curves for all elements are included in Appendix C.

High frequency roll-off, low frequency roll-off, and 3 dB bandwidth for each hydrophone gain response curve are presented in Table 2. Table 3 includes the corresponding frequencies associated with the high and low frequency roll-off. In each instance in which the data of Appendix C show response changes, due to dry out or other effects, between the 4th and 5th EY there is a recognizable change in one or more of the three parameters in the table.

2.2   Hardness and IR Data

The Shore A hardness data, averaged over all elements, are shown in Figure 6. The polyurethane molding of the elements demonstrated a very high Shore A value which was not impacted by the ALT.

The insulation resistance data for elements H15 and H7 are shown in Figures 7a and 7b. The following comments apply to the IR data in general, and can be seen in the plots of Figures 7a and 7b:

1.   Those elements which had dramatic changes in hydrophone gain response due to the dry out sequence between EY 4 and EY 5 also showed a dramatic High/Low air IR decrease prior to EY 4 followed by an increase in High/Low air IR between EY 4 and EY 5. This is another indication that these elements suffered at least partial loss of watertight integrity by the end of EY 4.
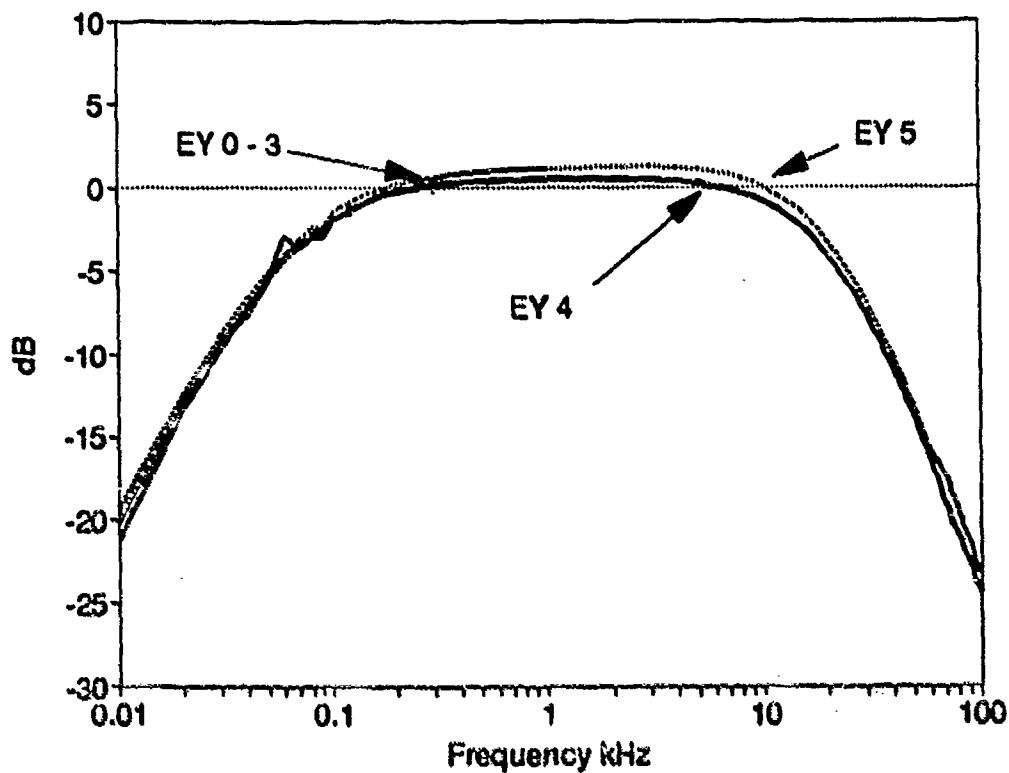
Figure 4. Hydrophone Gain Response Curves for Element H2
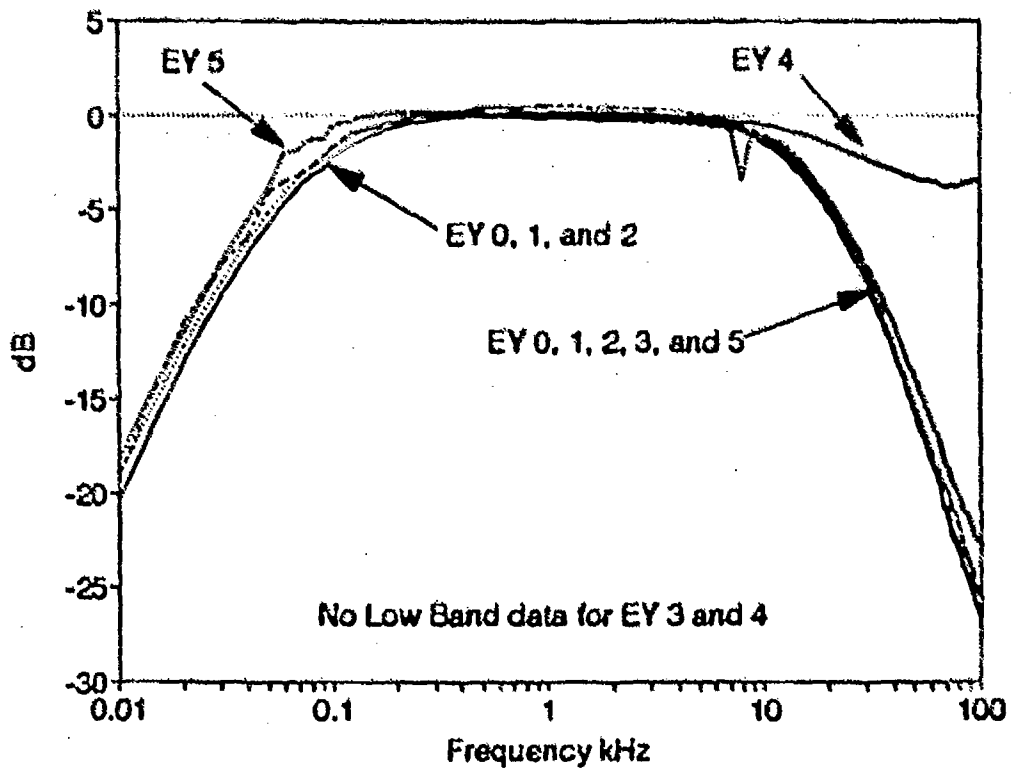
Figure 5. Hydrophone Gain Response Curves for Element H10

Table 2. High Frequency Roll-off, Low Frequency Roll-off, and 3 dB Bandwidth for Each Hydrophone Gain Response Curve

LF Roll-off (dB/Octave)

S/N	Equivalent Years					
	0.0	1.0	2.0	3.0	4.0	5.0
H1	6.47	6.14	6.07	6.43	5.56	6.12
H2	6.64	6.12	6.32	6.17	6.85	6.30
H3	6.51	6.24	6.28	6.71	6.40	6.27
H4	6.19	6.14	5.88	7.00	6.58	5.99
H5	6.49	6.21	6.21	7.00	6.54	6.36
H6	6.34	6.13	6.36	7.57	7.34	6.07
H7	6.09	6.26	6.56			
H8	6.31	6.28	6.39	6.98	8.63	6.46
H9	6.13		6.45	6.90	5.82	6.36
H10	6.47	6.14	6.25			6.31
H11	6.50	6.25	6.52	6.26	7.27	5.90
H12	6.27	6.13	6.41	6.44	6.49	6.16
H13	6.82	6.30	6.68	6.76	6.35	6.35
H14	6.43	6.29	6.68	6.73	6.59	6.44
H15	6.47	6.30	6.25			
H16	6.55	6.28	6.42	7.14	6.16	6.01
H17	6.61	6.25	6.47	9.05	6.49	6.40
H18	6.65	6.29	6.49	9.28	6.98	6.47
H19	6.68	6.37	6.49	6.67	6.33	6.41
H20	6.47	6.46	6.43	7.04	6.61	6.26
AVG	6.46	6.24	6.38	7.07	6.65	6.26
STDS	0.19	0.09	0.19	0.86	0.68	0.17

HF Roll-off (dB/Octave)

S/N	Equivalent Years					
	0.0	1.0	2.0	3.0	4.0	5.0
H1	10.95	10.90	10.87	10.42	8.75	10.57
H2	10.61	10.65	10.53	10.55	10.44	9.94
H3	10.55	10.62	10.53	10.55	10.36	10.15
H4	10.57	10.50	10.54	10.57	10.47	10.26
H5	10.85	10.48	10.82	10.59	6.98	5.99
H6	10.87	10.84	10.83	10.79	7.16	8.36
H7	8.77	9.36	10.81	6.77	2.58	10.31
H8	10.86	10.85	10.77	10.62	8.28	10.51
H9	10.89	10.89	10.88	10.79	10.70	10.47
H10	10.95	10.90	10.87	8.88		10.36
H11	10.90	10.90	10.88	9.75	9.10	10.58
H12	10.65	10.64	10.64	10.66	10.68	10.70
H13	10.75	10.74	10.74	10.20	10.70	10.46
H14	10.93	10.89	10.88	10.86	12.11	10.86
H15	10.91	10.83	10.87			
H16	10.90	10.89	10.85	10.89	12.11	10.63
H17	10.97	10.77	10.90	10.98	10.78	10.51
H18	10.85	10.81	10.78	10.90	10.91	10.36
H19	10.77	10.72	10.71	10.73	7.21	9.18
H20	10.78	10.76	10.76	10.73	3.22	7.73
AVG	10.71	10.70	10.77	10.33	9.15	9.89
STDS	0.48	0.34	0.12	0.99	2.51	1.25

3dB Bandwidth (Hz)

S/N	Equivalent Years					
	0.0	1.0	2.0	3.0	4.0	5.0
H1	14016	13804	13094	13371	14797	14282
H2	15231	15428	15251	15233	15365	15671
H3	14998	15076	14927	15166	15276	15345
H4	15467	14986	14933	15131	15300	16067
H5	13819	13818	13842	13502	20722	19244
H6	13931	13926	13903	13895	20515	17019
H7	19792	18559	14449	14870		13077
H8	13939	14150	14179	14951	14755	12597
H9	15660	13943	13659	14116	14502	14392
H10	14016	13804	13570	16061		15644
H11	13859	13947	13561	13359	20207	13966
H12	13764	13798	13789	13743	12030	13791
H13	14126	14336	13545	15913	12254	14234
H14	14097	14310	13405	14238	11116	14061
H15	13792	13778	13573			
H16	14148	14105	14061	13999	8805	14302
H17	13923	14017	13917	14052	12780	13996
H18	14431	14435	14336	14321	14474	15277
H19	13919	14026	13861	14489	14393	18298
H20	14060	14015	13993	14488	19818	20159
AVG	14451	14413	14022	14471	15118	15295
STDS	1351	1081	535	794	3438	2100

Table 3. Frequencies Associated with the High and Low Frequency Roll-off

Frequency at 3dB Low (Hz)

S/N	Equivalent Years					
	0.0	1.0	2.0	3.0	4.0	5.0
H1	91.16	83.88	85.67	90.81	87.37	84.95
H2	90.94	91.47	92.14	95.24	94.63	97.56
H3	94.10	87.50	84.46	96.62	95.92	96.52
H4	98.96	87.54	87.88	98.18	96.12	103.83
H5	87.41	83.05	81.70	79.12	91.48	98.43
H6	90.09	87.23	88.30	94.14	144.48	97.08
H7	90.68	84.38	85.10	97.25	251.95	88.13
H8	87.97	90.28	90.16	96.55	125.64	98.05
H9	80.78		79.98	79.19	91.96	87.44
H10	91.16	83.88	86.36			55.50
H11	88.66	88.01	84.52	53.62	107.38	93.44
H12	84.79	81.67	82.88	91.17	91.60	90.90
H13	92.63	85.00	83.58	94.45	92.68	93.41
H14	97.46	91.53	83.58	94.99	98.13	94.60
H15	90.11	86.31	86.39			
H16	94.47	86.01	85.32	94.19	96.82	92.71
H17	90.86	89.76	92.04	140.87	94.68	94.85
H18	96.28	88.72	79.97	124.57	95.98	95.07
H19	93.73	92.34	92.11	93.91	95.69	98.00
H20	91.68	90.51	90.55	94.65	97.68	94.95
AVG	91.20	87.32	86.13	94.97	108.34	92.39
STDS	4.21	3.15	3.82	17.57	38.42	9.96

Frequency at 3dB High (Hz)

S/N	Equivalent Years					
	0.0	1.0	2.0	3.0	4.0	5.0
H1	14107	13888	13180	13462	14884	14367
H2	15322	15520	15343	15328	15460	15768
H3	15092	15164	15012	15263	15372	15441
H4	15698	15074	15021	15229	15296	16171
H5	13907	13901	13924	13581	20814	19342
H6	14022	14013	13992	13989	20659	17116
H7	19882	18644	14534	14967		13165
H8	14027	14240	14270	15048	14880	12685
H9	13741	13943	13739	14196	14594	14480
H10	14107	13888	13657	43600	16081	15900
H11	13978	14035	13945	13443	20315	13060
H12	13849	13980	13872	13834	12119	13882
H13	14219	14421	13929	16008	12347	14327
H14	14194	14401	13489	14333	11204	14156
H15	13883	13859	13659			
H16	14243	14191	14147	14093	8902	14395
H17	14022	14134	14013	14193	12875	14091
H18	14527	14524	14416	14458	14570	15372
H19	14013	14118	13953	14572	14489	18401
H20	14152	14106	14084	14583	19905	20254
AVG	14549	14497	14109	16009	15265	15388
STDS	1355	1082	536	6718	3348	2102

Figure 6. Average Shore A Hardness for All Elements
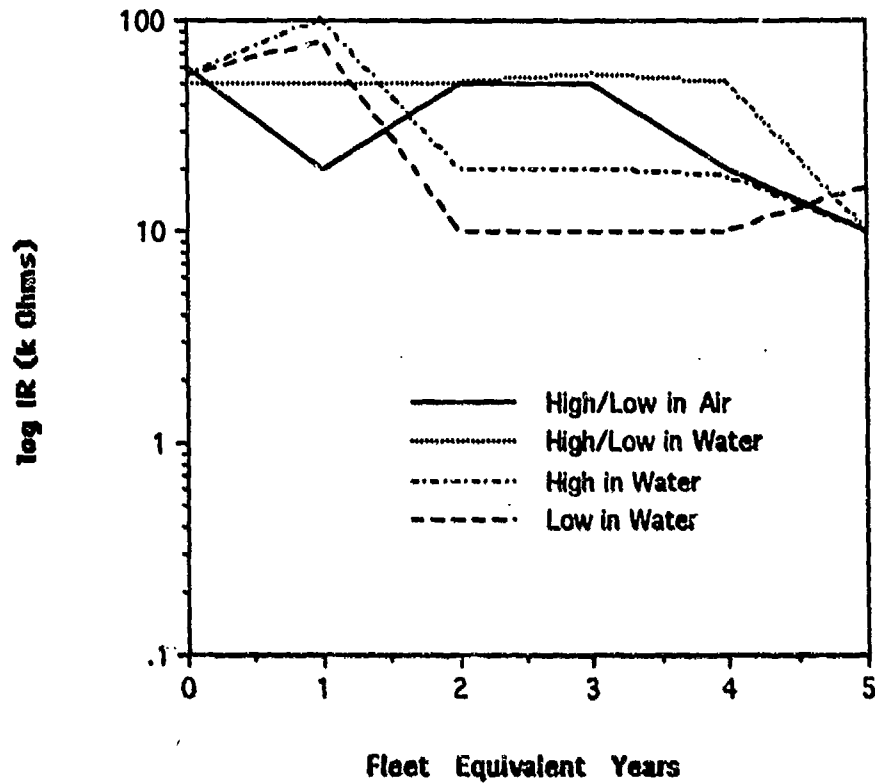
Figure 7a. IR Data for Element H15
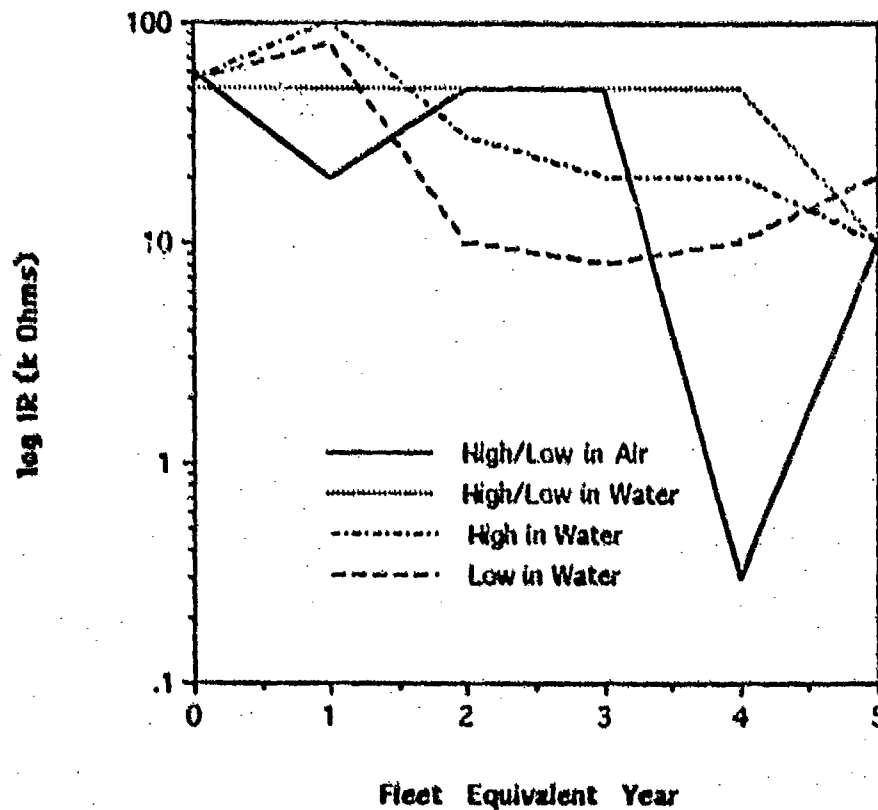
Figure 7b. IR Data for Element H7

2. The low side IR in water tended to decrease somewhat between EY 1 and EY 2 and recovered between EY 4 and EY 5 for all elements. This is fairly typical IR behavior for ALT units – an early decrease in IR which shows improvement after a dry out cycle. This is different than the situation above in which a much more dramatic change is observed that is correlated with ingression into the unit for its conductors.

3. The High side in water data showed a small decrease between EY 1 and EY 2 and decreased somewhat between EY 4 and EY 5. The High/Low water IR was similar for those elements which had no watertight integrity problem.

2.3   CUALT Data Summary

A qualitative summary of the ALT data for each element grouped by common attribute is:

- Elements With No Problems: H2, H3, H4, H9, H17, and H18
- Elements With Dry Out Recovery: H1, H8, H11, H12, H13, H14, and H16
- Elements With No Dry Out Recovery: H5, H6, H19, and H20
- Elements With Anomalous Gains: H7, H10, and H15

The first grouping is composed of elements which experienced no problems during the CUALT. The second group had gain anomalies (e.g., bandwidth decrease in EY 4 for elements H12, H13, H14, and H16, roll-off decreases which returned to initial value for elements H1, H8 and H11) which were corrected by the dry out period between EY 4 and EY 5. The third group had EY 4 and EY 5 gain anomalies (all four of these had increases in EY 4 and EY 5 bandwidth with associated decreases in roll-off), while the last three elements had anomalous data which involved changes in the shape of the hydrophone gain curves.

Due to these anomalies, elements H7, H10 and H15 are cause for concern.

Since there were only six elements which had no problems during the term of the test (70% failure rate), there appears to be a design limitation for the prototype HGA elements to achieve a service life goal of five years. At least seven elements, and possibly as many as 11 elements (second and third groups above) showed evidence of moisture ingression into the hydrophone or the conductors for those elements. This could be a workmanship issue, a material selection problem, or even a condensation issue, and design modifications have been made to correct this problem in the production (as opposed to prototype) run of the HGA staves.

It should be noted that bandwidth and roll-off data of Table 2 appear to be sensitive indicators of problems for the HGA elements. It may be worthwhile to compute these periodically in service using the gain measurement calibration mode to determine array health.

3.0   HIGH GAIN ARRAY STAVE AUTOPSY

After being subjected to five equivalent years of CUALT, the HGA stave was delivered to TRI/Austin for disassembly and degradation analysis, or autopsy. Due to the complexity of each of the twenty hydrophone elements and time constraints, complete disassembly was not accomplished for each element. Instead, objectives were identified to characterize significant configuration items, primarily on a representative basis. However, in the case of evaluating EMI shielding of the hydrophones' aluminum spools, all elements were subjected to electrical continuity testing.

3.1   Visual Observations and Preliminary Electrical Testing

The HGA stave was previously shown in Figure 1 as received for autopsy. Three of the hydrophones (H1, H13, and H19) were observed to have been coated with a black paint, but only residual coating remained at the time of autopsy. Average residual coating was estimated to be less than 50 percent overall. The paint was applied during the third EY of CUALT.

Copper mesh shielding was observed to be encapsulated within the molded boots of 11 of the hydrophones: all even numbered units plus H11. Nine of the hydrophones were shielded with a similar copper mesh stranding. Serial number H11 was observed to have a woven mesh formed with interlocking loops. The copper shield of H16 was coated with a black polymeric material. Discussions of shield configuration and EMI functional evaluations are detailed in the following section.

Each of the hydrophones was observed to have been overbooted with an amber polyurethane molding compound. The printed circuit boards of each hydrophone were visibly pre-potted in polyurethane molding compound within the potting of the outer boot. The ceramic stack assembly was specified to be pre-potted also; however, the molding was not visible through the outer boot. According to DWG. NO. 050491.DWG, the ceramic was pre-potted with Hexcel Corp. 185N. The outer boot molding was not identified during autopsy but was observed during CUALT to have a nominal Shore A hardness of 94-96, which suggests that it was probably the same Hexcel 185N. (This might also explain why the pre-potting of the ceramic was not visible, since identical molding compounds often do not provide contrast when encapsulations merge.) The PCB potting material was specified (DWG. NO. 050591.DWG) to be Products Research and Chemical Corporation's PR-1547, which has a nominal Shore A hardness of approximately 75.

Each hydrophone was also observed to have been repaired after final boot molding as evidenced by an obvious site of excavation and filling with polyurethane compound. The repair sites were all located adjacent to the opening of the "U" in the printed circuit board.

No serial numbers were visible on the connector or on either of the end terminations, as required by the "Hydrophone Stave Requirements/Specifications."

3.2   EMI Shield Evaluation

According to the table of DWG. NO. 050291.DWG, all of the odd numbered hydrophones are specified to be unshielded. A discrepancy was noted for element H11 which was found to be shielded. Although the unshielded units were not instrumented with a copper sleeve, the aluminum spools were intended to be wired to the stave's ground circuit to provide EMI isolation of the ceramic elements from the feedthrough wiring bundle.

Small cavities were excavated into the boot moldings with a high-speed grinding tool to gain access to the shield, spool, and wiring components. For all the units, the surface of the spool was ground with a Dremel tool to remove the anodized (non-conductive, aluminum oxide) coating. Continuity testing was conducted using a Fluke Model 77 digital voltmeter to characterize EMI shielding integrity. Initial site selection for testing shield-to-spool continuity was in error due to the inclusion of a 0.1 microfarad capacitor in the circuit. (The capacitor is directly attached to the shield of the primary coaxial conductor for each element.) As expected, testing with the capacitor in-line resulted in measurements of open circuits in all cases. Repeated testing was performed with an alternate site selection which accessed the lead between the capacitor and the aluminum spool.

As shown in Table 4, 12 of the 20 elements were found to have open or intermittent shield circuits between the aluminum spool and the coaxial wire shield. The attachment of the capacitor lead to the spool was made by an adhesive bond with Masterbond BP76M, reported to be a nickel impregnated conductive epoxy.

Table 4. Aluminum Spool Continuity Test Results

1 OPEN	6 OPEN	11 OPEN	16 5 MΩ
2 OPEN	7 OPEN	12 OPEN	17 INTERMITTENT
3 12 MΩ	8 400 Ω	13 OPEN	18 600 Ω
4 70 Ω	9 16 MΩ	14 5 MΩ	19 30 MΩ
5 OPEN	10 OPEN	15 OPEN	20 OPEN

Five of the elements (H1, H5, H10, H15 and H19) were carefully inspected at the site of lead attachment to the spool. The boot molding compound was removed from around the lead and the edge of the spool. Continuity measurements between the ground surface of the spool and the lead directly above the bonded attachment confirmed open circuits. Two of the leads appeared to be tightly bonded (H5 and H19) and were the only ones configured with a build-up, or fillet, of epoxy around the penetration.

The conductor leads were then removed from the attachment site and the epoxy was tested. A needle attached to a probe of the digital voltmeter was inserted in each hole and resistance was measured to the bared aluminum surface. Open circuit measurements clearly indicated that the epoxy was non-conductive at the time of autopsy. Additionally, two needle probes were placed adjacently across the surface of the epoxy within the holes on two hydrophones, and again open circuits indicated a lack of surface conductivity.

The epoxy was observed to be black, and in four units apparently rigid throughout. However, some of the material removed from the spool of H5 was soft, apparently due to either an incomplete cure, contamination from the boot molding operation, or other causes. After material was removed from the inside surfaces of the drilled holes, resistance was measured with the needle probe from there to the ground area of the spool. Continuity was confirmed, which suggests that the drilled holes were properly made after the spools were anodized.

Wiring circuits and soldered connections to the copper mesh sleeves were found to be functional in all shielded elements.

3.3   Outer Boot Molding

The hydrophone assemblies were configured with a minimum of three separate polyurethane molding operations. The printed circuit board and ceramic stack/spool assemblies were pre-potted prior to hydrophone construction and then encapsulated within an outer boot. In addition, each of the twenty hydrophones were observed to have distinct repair sites (obviously unplanned) made apparently to correct electrical wiring deficiencies involving circuit attachments of the PCB assembly. This procedure apparently required excavation into the boot molding, circuit repair, and re-enclosure of the site with an injection of molding compound to reconfigure the outer boot. The exact nature of the repair was not determined during autopsy.

3.3.1   PCB Pre-potted Subassembly

The pre-potted molding subassembly of the PCB of the hydrophone was characterized by autopsy inspections of five units. According to DWG. NO. 050591.DWG, the pre-potting should have formed a uniform wall thickness around the "U" cut-out of the PCB. However, in each of the units which were inspected, the wall thickness of the molding decreased significantly in the radius of the "U." The thickness was approximately 0.006 inches on one unit and may have decreased to near zero in two others. A cross-sectional view of the PCB of H19 is shown in Figure 8.

The pre-potted PCB moldings appeared to be generally free of voids and air bubbles.

Figure 8. Pre-potted PCB Assembly Tinted with Red Ink

3.3.2 Ceramic Stack Pre-potted Subassembly

The pre-potted moldings of the ceramic appeared to be generally free of voids and air bubbles.

3.3.3 Outer Boot Molding

The outer boot moldings were observed to vary in quality from unit to unit; however, many were affected by air bubbles and other molding defects. In general, there were more bubbles in the area of the PCB, although some units had bubbles trapped in the shield sleeves over the ceramic elements. Other defects included sites of cloudy (or opaque) material, which may suggest poorly mixed catalyst and resin of the molding compound. The repair sites made to correct electrical defects were all observed to have numerous air bubbles and many had cloudy sites. This is not considered unusual, however, since wiring repairs involving molten solder and possibly solder flux would be difficult to perform without residual contamination.

3.4 Wiring Inspection

The wiring harness bundle was inspected at various sites along the length of the stave. It was noted that there were 30 wires in the bundle and there was a tendency for the jacket insulation to discolor from gray to yellow along the length of the stave. Between the electrical connector and element H1 there were six wires which were distinctly yellow, eight which were slightly discolored, and 16 which were gray (as specified). Beyond H20, there were only eight wires which were gray, three slightly discolored, and the rest distinctly yellow. Inspections of the shield and conductor strands of the coaxial leads suggested that there was a correlation between

discoloration and the presence of corrosion products around the copper stranding. This would suggest that water and resulting corrosion products caused the observed discoloration. Figure 9 shows the wiring bundle laid flat and in numerical order top-to-bottom. The upper bundle was taken between the connector and H1 and the lower was from a section past H20.

Figure 10 shows a yellowed and a gray conductor. Note that the shield of the yellowed conductor is severely corroded and exhibits a red, pasty corrosion product. Other corroded shields had a black, powdery corrosion product.

The yellow discoloration was not necessarily gradual or uniform for any given wire. In some cases, mottling occurred and jackets were seen to change color abruptly and repeatedly through a given length between hydrophones. It is suggested that the increasing number of yellowed conductor jackets toward the end of the stave is related to the increasing number of opened conductors along the stave. It was noted that as conductors were used in the hydrophone circuits, a loose end of the wire was found between the hydrophone in which it was used and the next one in series. This allowed the overall bundle size to remain constant throughout the stave, but also produced an increasing number of conductors that were open to water.

A color code for the 24 coaxial conductors of the wiring bundle is included in note 1.C. of DWG. NO. 050191.DWG. A discrepancy was noted during autopsies involving wire numbers 21 and 24. Assuming that the listing shown in the table implies numerical order, the yellow/brown and yellow/green wires were reversed.

Water was observed between the outer insulation (reported to be a product referred to as MIL-ENE® C rated at 300V) and the gray polyurethane jacket on many conductors. Probable entry sites were identified near many of the hydrophones, where the MIL-ENE® insulation was found to be distorted (wrinkled), apparently due to flexing caused by handling. In the worst cases, fatigue resulted in breaks in the insulation. Figure 11 shows two conductors with damaged insulation and water between the insulation and jacket.

Water droplets were found on conductors within the hydrophone encapsulations of three units (H7, H15, and H19), as verified by insertion and removal of a needle which resulted in water migration out of the resultant hole.

3.5   Tensile Testing of Center Strength Member

The wiring harness bundle used in the HGA is configured with an inner strength member of 3/16 in. nominal diameter composed of an outer, braided sleeve (material unidentified but possibly nylon) and an inner core of Kevlar®. Tensile testing was performed on three lengths of the strength member using an Instron universal testing machine. Overhand knots were tied into the ends of each segment which were used to affix the cords around 0.5 inch steel pins. Failures occurred at 1340, 960, and 1380 pounds of axial load (for an average of 1227 pounds). Breakage occurred near, but not within, one of the knots during each test.

Figure 9. Wiring Bundles Removed from Either End of the Stave

Figure 10. Corrosion Products in Yellowed Conductor
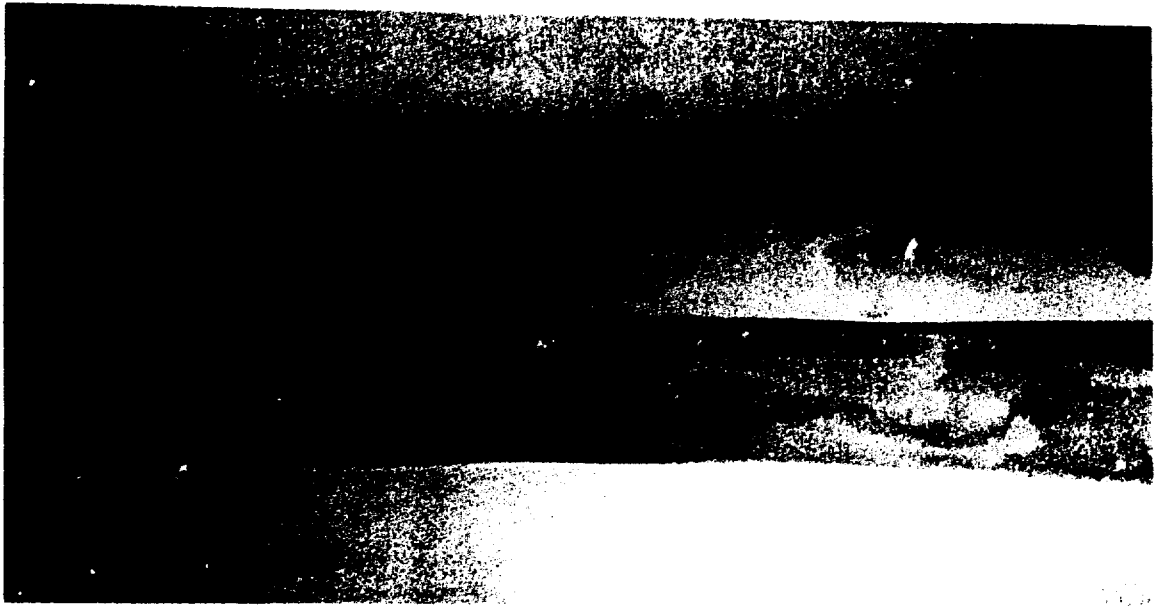
Figure 11. Water Present Between Degraded Insulation

4.0   SUMMARY OF AUTOPSY FINDINGS

The most significant observations made during the HGA stave autopsies are summarized below:

- EMI shieldings of the aluminum spools were found to be flawed by the lack of conductivity of the epoxy used to bond the capacitor leads. In addition, the epoxy failed to provide a tight bond of the leads, perhaps due to shrinkage or a basic incompatibility with the copper lead.

- Deficiencies were observed with the positioning of the printed circuit boards within the pre-potted polyurethane moldings. In the worst case (H15), there appeared to be an area in the radius of the "U" cut-out where there was practically no coverage of the edge of the board. In H10, the thickness at one site of the radius was approximately 0.006 inches and on H19 the material decreased to near zero thickness.

- Water was found between the outer insulation and the jacket of many of the coaxial stave wires. In addition, the insulation was found to be distorted, or wrinkled, in numerous sites near entry and exit sites of individual hydrophone elements. (No damage was observed in areas away from hydrophones.) In some cases, the wrinkled sites were open, apparently due to cyclical fatigue due to bending. It is suspected that these degraded sites provided the leak path for water ingression along the wiring bundle.

- Water droplets were also observed on various wires and terminations within several hydrophone elements. It is suspected that wicking occurred along the coaxial wires between the outer insulation and the jacket.

- Many of the hydrophones had poor outer boot moldings, especially in the area around the pre-potted PCB. The pre-potted moldings of the PCB and ceramic cylinders were generally free of voids. In addition to the bubbles, many of the outer moldings were affected by discolored sites which appeared to be due to incomplete mixing of the catalyst and resin of the polyurethane molding compound. Areas were also found where the material within the boots was very soft and apparently in the "gum" state, or incompletely cured.

- Many insulation jackets in the 30-conductor wiring bundle were observed to have discolored from gray to yellow. Inspections revealed that at the connector end of the bundle, 14 of the jackets showed at least some yellowing, but that only six of these were completely yellow. At the area beyond element H20, however, only eight of 30 conductors remained gray. There appeared to be a correlation between the discoloration and corrosion products and moisture in the conductor strands.

- The shields of the discolored coaxial leads were observed to be most severely degraded (in both numbers and degree) in increasing extent from the middle of the stave to beyond element H20. The worst shields were found to have a red, pasty substance in the interstices between strands. It was not determined whether this was a corrosion product of the copper strands or a material which migrated along the conductor. The discoloration and shield degradation may also be related to the increasing number of open conductors within the bundle towards the end of the stave.

Appendix D contains various representative photographs taken during the HGA stave autopsies.

APPENDIX A

MISSION PROFILE FOR NSWC HGA POTTED HYDROPHONE STAVES

1.   <u>Shipment</u>: The staves will be shipped/stored on individual reels with an inner diameter of one foot.

2.   <u>Installation</u>: The staves will be installed vertically on the HGA frame and each stave will be tensioned to a nominal load of 150 pounds.

3.   <u>Storage</u>: The HGA modules will be stored on the deck of HAYES and exposed to the environment (sunlight, salt spray, wind, etc.). The HGA modules may be designed to be collapsible in the storage mode. In this case, the staves would remain attached to the frame but would undergo some bending and redistribution.

4a.   <u>East Coast: Deployment</u>: The HGA modules will be deployed via a crane and winch and slowly lowered to the appropriate depth. Two HGA modules will be deployed at a nominal depth of 400 feet. The third module will be deployed through the center well of the HAYES. The depth of this module will be varied from 400 feet to 1600 feet. During this period of deployment, the modules may be towed through the water at speeds up to 3 knots as the HAYES repositions itself due to changes in wind direction. Water temperature may vary from 55°F to 85°F.

4b.   <u>West Coast: Deployment</u>: The module will be deployed and anchored to the ocean bottom. The water depth will be 400 feet and the nominal water temperature is 42°F.

5.   <u>Duration</u>: For the East Coast Trials Program, typical trials are one week in duration with approximately 24 trials per year. For the West Coast Trials Program, the module will remain anchored to the ocean bottom on a semi-permanent basis.

APPENDIX B

RELIABILITY TESTING OF LONG LIFE UNDERWATER COMPONENTS

RELIABILITY TESTING OF LONG LIFE UNDERWATER COMPONENTS

Alan V. Bray and Shawn L. Arnett

Texas Research Institute Austin, Inc.
9063 Bee Caves Road
Austin, Texas 78733

ABSTRACT

Real time reliability testing for long life components is expensive and the testing period often precludes corrective action before service use. Accelerated life testing (ALT) is a common method for assessing the reliability of electronic components, but classic electronic ALT methods are not applicable to submerged components. Methods for quantitative ALT of underwater components with acceleration factors ranging from seven (7) to fifteen (15) equivalent Fleet service years per calendar year of test are discussed. The acceleration factor is dependent upon the mission profile the component experiences in service. Recently developed techniques for estimating the Fleet service life of underwater components from ALT are presented. Examples of transducer and connector reliability tests are presented to illustrate the methods. Reliability estimation from ALT results in test-to-failure and test-to-degradation designs are discussed.

INTRODUCTION

Acceleration of the service stresses to which a component is subjected is done in two ways; duty cycle acceleration and stress intensity acceleration. Duty cycle acceleration involves subjecting the component to service stresses for a time period which exceeds normal service durations. A component which is submerged in salt water for eight (8) hours a day in service can be tested with a duty cycle acceleration factor of three (3) by submerging the component 24 hours a day.

Stress intensity acceleration involves the application of a higher stress to the component than it will experience in service. As an example consider corrosion, in which the rate of degradation is accelerated by increasing temperature. For a submerged component whose failure rate is proportional to extent of corrosion, reliability testing at elevated temperatures will corrode, and then fail, the part faster. Mathematically one can depict this as a translation of the time scale of the reliability function of

the component, resulting in the linear acceleration assumption [1],

$$R_s(t_s) = R_a(t_s A) \tag{1}$$

where R_s is the reliability in normal service use and R_a is the reliability under an accelerated stress condition. The linear acceleration factor, A, relates time to failure at accelerated stress (t_a) to time to failure under normal service (t_s).

SUBMERGED COMPONENT ALT

Common submerged components such as connectors, transducers, underwater cameras, cables, hulls, and so on, can be tested for reliability in a fraction of the expected life of the item by proper use of the relationship in (1). Stresses to which submerged components are routinely exposed include temperature, temperature cycling, pressure, pressure cycling, electrochemical reactions (often accelerated by temperature increases), and air exposure stresses prior to installation or during maintenance which include sunlight (UV), temperature, humidity, and air pollution. Additional stresses include those associated with actual operation such as the pulsing of a piezoelectric transducer or the load on an ROV drive motor.

Designing an ALT schedule requires characterization of the mission or use profile into the stresses and durations experienced in service. An example [2] of this is shown in Figure 1 which is a portion of the mission profile for the TR-317, the AN/BQQ-5 Spherical Array transducer. For each stress in the components' mission profile one or more acceleration factors are taken into account. As an example, the acceleration factor for temperature comes from the Arrhenius equation for thermal stress aging, and time to failure (t_f) is given by

$$t_f = B \exp\left(\frac{a}{kT}\right) \tag{2}$$

where B is a constant, a is the activation energy associated with the thermal aging process which is dependent on the specific material, r is Boltzmann's constant, and T is the temperature in degrees Kelvin. The acceleration factor between service and laboratory test temperatures is the ratio of the times to failure at the two temperatures,

$$A = \frac{B \exp\left(\frac{a}{rT_s}\right)}{B \exp\left(\frac{a}{rT_l}\right)} = \exp\left[\frac{a}{r}\left(\frac{1}{T_s} - \frac{1}{T_l}\right)\right] \qquad (3)$$

Mission Profile - Service Mode TR-317			
Exposure	Occurrence	Extreme Duration	Long Term Duration
Temperature	Tropical	+32°C 960 hrs./yr.	7°C - 21°C 3420 hrs./yrs.
Sea Water	Arctic	-2°C 960 hrs./yr.	-1 to 11°C 3420 hrs./yrs.
⋮	⋮	⋮	⋮

ALT Plan Calculations		
Service Duration	Acceleration Factor A	ALT Duration (t_A)
32°C/960 hrs.	11.47	159 hrs. @ 70°C Tropical
14°C/3420 hrs.	45.66	
-2°C/960 hrs.	181.82	41 hrs. @ 70°C Arctic
5°C/3420 hrs.	97.09	
⋮	⋮	⋮

FIG. 1 AN ILLUSTRATION OF MISSION PROFILE TRANSLATION INTO ALT PLAN FOR THE TR-317

The value of A in equation 3 is always greater than one for laboratory temperatures which are greater than service temperatures, and this is an example of why the reliability of a component can be measured in less than real time. Similar acceleration factors are used for the other stresses, and the final ALT design is a linear programming problem to balance the accelerated exposure times with the mission profile.

Pressure cycling acceleration factors are associated with fracture failure modes resulting from material cyclic fatigue. The crack growth process in these fracture failure modes is proportional to pressure differential raised to the fourth power for many polymeric materials. The acceleration factor is then the fourth power of the ratio of the laboratory and service cyclic pressure differentials, i.e. $(\Delta P_l/\Delta P_s)^4$.

The laboratory tests which make up an ALT are component mission profile stresses at durations and levels determined by the physical acceleration factors. Each material and sub-component must be assessed for its response to the service stress profile and included in the ALT plan. The result is a series of laboratory exposures which represent an equivalent year of Fleet use. Testing consists of exposing the item to the ALT schedule and measuring the performance of the component as a function of Fleet equivalent time.

The total acceleration factor in equation (1) is the ratio of the ALT exposure time to the to the Fleet use time being accelerated. In the case of an item with an expected Fleet life of fifteen (15) years and a test time of 1.5 years of actual exposure, A is ten (10). The figure of merit for the cost benefits of an ALT is .ne ratio of total laboratory test time, (including diagnostic measurement time, dead times associated with logging the transducers into the laboratory, and similar periods) to Fleet lifetime. Handling overhead adds approximately 10% in calendar time at the two NRL/USRD sponsored ALT facilities in Austin, Texas and Orlando, Florida. The efficiency of the tests for Navy ship/submarine wet end components ranges from 7.0 to 15.0 depending on the item tested and its mission profile.

EXAMPLE TEST RESULTS AND ANALYSIS

In tests which continue until all of the units have failed, the unit failure rate, reliability, and MTBF are estimated based on the time of failure. An example is shown in Figure 2 for the standard MIL-C-24231 connector used in the AN/BQR-7 sonar system. Also shown in the figure is data from a specific submarine. The data presented is the reliability based on the Fleet disconnect criteria for the insulation resistance (IR) of the connector as a function of Fleet equivalent years of service. Material hardness and pin-to-pin capacitance are usually also monitored in connector ALT, but the IR data suffice for example. Both data sets are presented in terms of reliability as a function of time, with the Fleet data analyzed by computing the percentage of operating units as a function of time, while the ALT data were analyzed using a non-parametric estimate for small sample size reliability tests given by [3]

$$R(t) = R(t_aA) = 1.0 - \frac{[n(t_aA) - 0.3]}{N + 0.4} \qquad (4)$$

Where the t_aA term is shown to illustrate that this is the equivalent Fleet reliability function, $n(t_aA)$ is the cumulative number of failures at Fleet equivalent time t_aA and N is the number of units in test.

AN/BQR-7 Hydrophone Connector Reliability
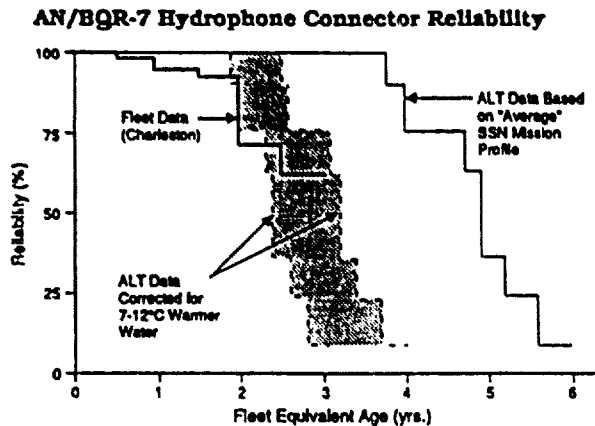
FIG. 2 A COMPARISON OF FLEET AND ALT RESULTS FOR THE MIL-C-24231 STANDARD CONNECTOR USED IN THE AN/BQR-7 SONAR

The ALT plan on which the laboratory tests were based was for an average submarine profile for units based in all ports [2]. The specific submarine used for the study was based in Charleston, S.C. in much warmer water than average. The primary failure mode for these connectors is cathodic delamination [4] of the polymer encapsulation material from the steel backshell of the connector, and this failure rate is accelerated by water temperature. The shaded region in Figure 2 shows the adjusted result had the ALT Plan been based on the warmer water exposure condition. This shows that the ALT scaling of the Fleet equivalent year was fairly accurate, and that ALT data are representative of the reliability of this connector in Fleet service. This connector has since been singled out for a higher reliability design which uses a glass reinforced epoxy composite backshell and eliminates the cathodic delamination failure mode [5].

In another recently completed test TR-317R transducers were subjected to a fifteen (15) Fleet equivalent year ALT. These transducers were expected to last fifteen years in terms of gross operability, but there was potential for aging degradation of the transducer parameters in Fleet use. The units underwent an ALT schedule similar to the connectors above, and immittance, IR and material measurements were made each equivalent year.

A set of degradation limits was deduced from the Critical Item Procurement Specification (CIPS) [6] and these provided the basis for estimating the reliability as a function of Fleet equivalent age.

Admittance resonance-frequency change data from the test units are shown in Figure 3. The data are the result of a spectral features algorithm which fits the admittance and displacement per volt spectra with a cubic spline. The analytic function which results is then examined for extremes which correspond to resonance frequencies; and the quality factor (Q) for each resonance is computed as the ratio of the 6 dB down peak width to the resonant frequency. These data are baseline corrected to their value in a new condition, i.e. for each measured spectral parameter the value C_i, where i is the time index, is referenced to time zero by

$$\Delta C_i(t_aA) = C_i - C_0 \qquad (5)$$

The ΔC_i data are then fit with a linear degradation function of the form

$$\Delta C_i(t_aA) = b + ct_aA \qquad (6)$$

ΔF1 Values
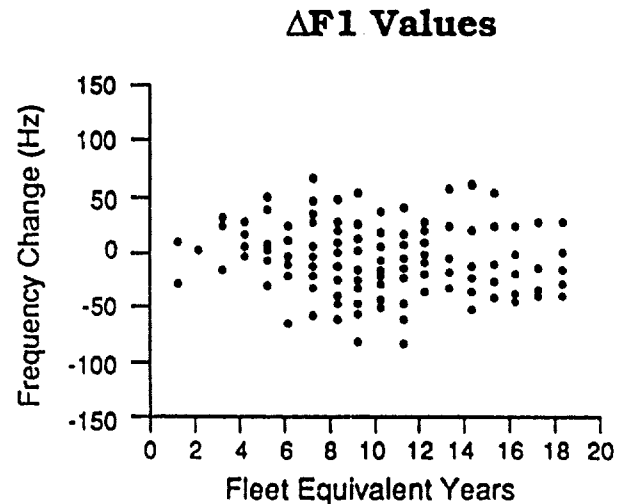
FIG. 3 BASELINE CORRECTED ADMITTANCE RESONANCE FREQUENCY MEASUREMENTS FOR THE TR-317R AS A FUNCTION OF FLEET AGE

This statistic is used to predict (for short periods beyond the ALT) the reliability of the transducer. This is accomplished using the probability density function (pdf) of the ΔC_t. Using the student t distribution for the pdf in a classic prediction problem [7] results in a critical value of t given by (the t_aA notation is dropped in 7 and 8 for clarity):

$$t_{crit} = \frac{\Delta C_{crit} - |b + ct|}{\hat{\sigma}\sqrt{\dfrac{n}{n-2}\left[\dfrac{n+1}{n} + \dfrac{(t_p - \bar{t})^2}{\sum_i (t_i - \bar{t})^2}\right]}} \quad (7)$$

where

$$\hat{\sigma} = \sqrt{\frac{\sum[\Delta C_i - (b + ct)]^2}{N}}, \quad (8)$$

ΔC_{crit} is the critical value for the parameter in question, i.e. the point at which the transducer parameter has degraded to a point which impacts function, and t_p is the time at which the prediction is made. This is illustrated in Figure 4.
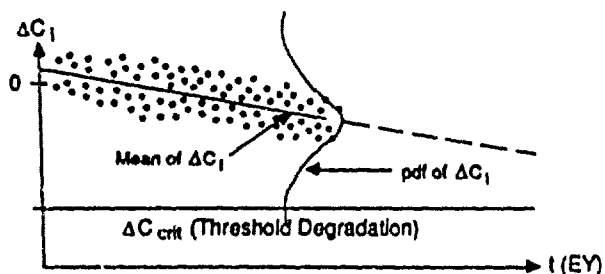
FIG. 4 ILLUSTRATION OF ANALYSIS OF SAMPLE DATA

The reliability function associated with the parameter C is then the probability that ΔC_{crit} is not exceeded. This is approximated as

$$R[C(t)] = \frac{1}{\sqrt{2\pi}}\int_{-\infty}^{t_{crit}} e^{-1/2t^2}\, dt \quad (9)$$

Equation nine (9) provides the reliability function associated with the jth reliability measure C_j.

Figure 5 shows the reliability function associated with the data shown in Figure 3, and also includes the control unit reliability processed in the same manner. In

addition sixteen (16) other measures were examined for degradation. Some examples include:

• Encapsulation hardness
• Admittance Resonance Q
• Cable and transducer capacitance
• Cable and transducer IR
• Housing resonance
• Admittance Resonance Magnitude
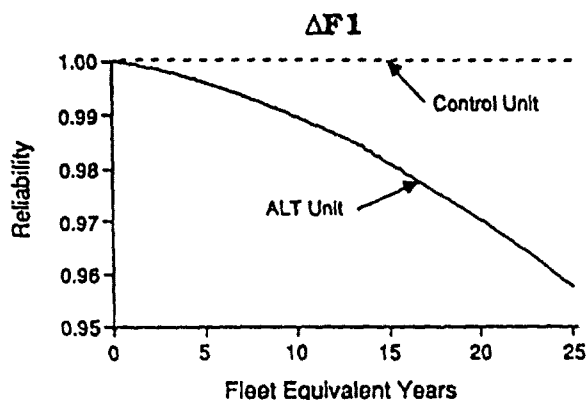
FIG. 5 THE RELIABILITY FUNCTION FOR THE DATA OF FIGURE 3 USING THE METHOD ILLUSTRATED IN FIGURE 4

The final estimate of TR-317R reliability is the product of the reliability functions for each of the component measure at each time increment, i.e.

$$R(t_aA) = \Pi R_j(t) \quad (10)$$

where the index j is over the individual reliability measures. There is admittedly an issue here regarding the independence of these estimates. Each R_j relates to a specified measure of degraded performance, but some may be degraded by the same failure/degradation mode as others. The impact of this effect is to provide a loose lower bound estimate of the reliability of the transducer. The resulting reliability estimate for the TR-317R transducer is shown in Figure 6 along with the control unit data processed in the same fashion. Also shown in the figure is the reliability specification criteria for this Fleet component, and from these data it is clear that the TR-317R satisfied the specification for reliability.

TR-317R Composite Unit Reliability
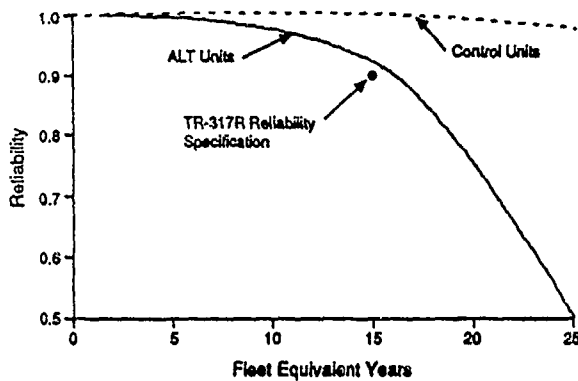
FIG. 6 FINAL ALT RELIABILITY ESTIMATE
FOR THE TR-317R TRANSDUCER

CONCLUSIONS

Verification of reliability specifications for long life underwater components is a difficult task in real time since flaws that limit product life may not be discovered until the government no longer has the contractural opportunity to correct them. In the procurement cycle the opportunity to verify reliability first presents itself at first article delivery, and the time frame between first article and acceptance is often large enough to complete an ALT and obtain quantitative measures of reliability. The ALT times required for submarine components is from 1 to 1.5 years for a complete mission profile test, and can be reduced for specific failure mode testing. Surface ship ALT times for long-life items range from 1 to 2 years for a complete mission profile test. Sub-components such as coatings and encapsulations can be tested in as little as 4 to 6 months. The methods have been proven to correlate well with Fleet data and represent the shortest time period for full term validation of reliability specifications.

ACKNOWLEDGEMENTS

REFERENCES

1. P.A. Tobias and D. Trindale, Applied Reliability, Van Norstrand Reinhold, New York, 1986.
2. R.W. Timme and J.F. Cartier (Ed.), "NAVSEA Transducer Improvement Program (NTIP) FY88 Third Quarter Progress", NRL Memorandum Report 6280, Work Unit IV.A.
3. K.C. Kapur and L.R. Lambertsom, Reliability in Engineering Design, Wiley, NY, 1977.
4. J.S. Thornton, R.S. Montgomery, and J.F. Cartier, "Failure Rate Model for Cathodic Delamination of Protective Coatings", NRL Memorandum Report 5584, May 30, 1985.
5. Sea Technology, April 1989, Vol. 30, No. 4, p. 41.
6. R.W. Timme and J.F. Cartier (Ed.), "NAVSEA Transducer Improvement Program (NTIP) FY88 Fourth Quarter Progress", NRL Memorandum Report 6371, Work Unit IV.B.
7. A.M. Mood and F.A. Graybill, Introduction to the Theory of Statistics, McGraw-Hill, New York, 1963.

APPENDIX C

RESPONSE CURVES FOR ALL ELEMENTS

EY 0, 1, 2, 3, and 5

EY 4

EY 4 Data corrected for dB shift

Element 1

EY 0 - 3

EY 5

EY 4
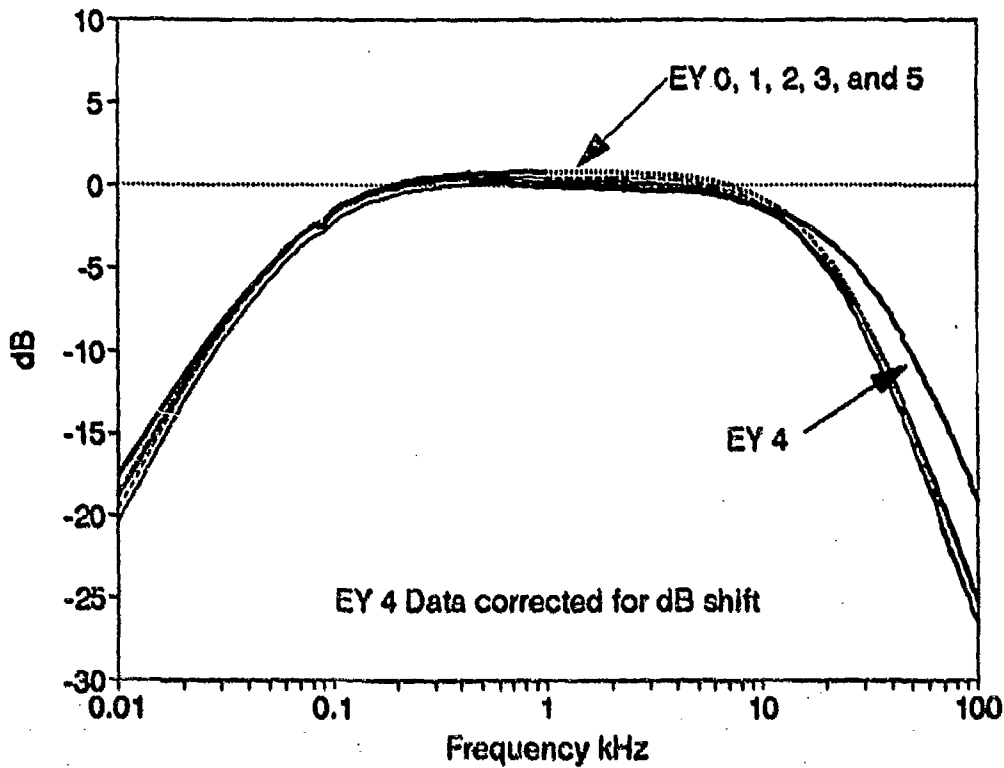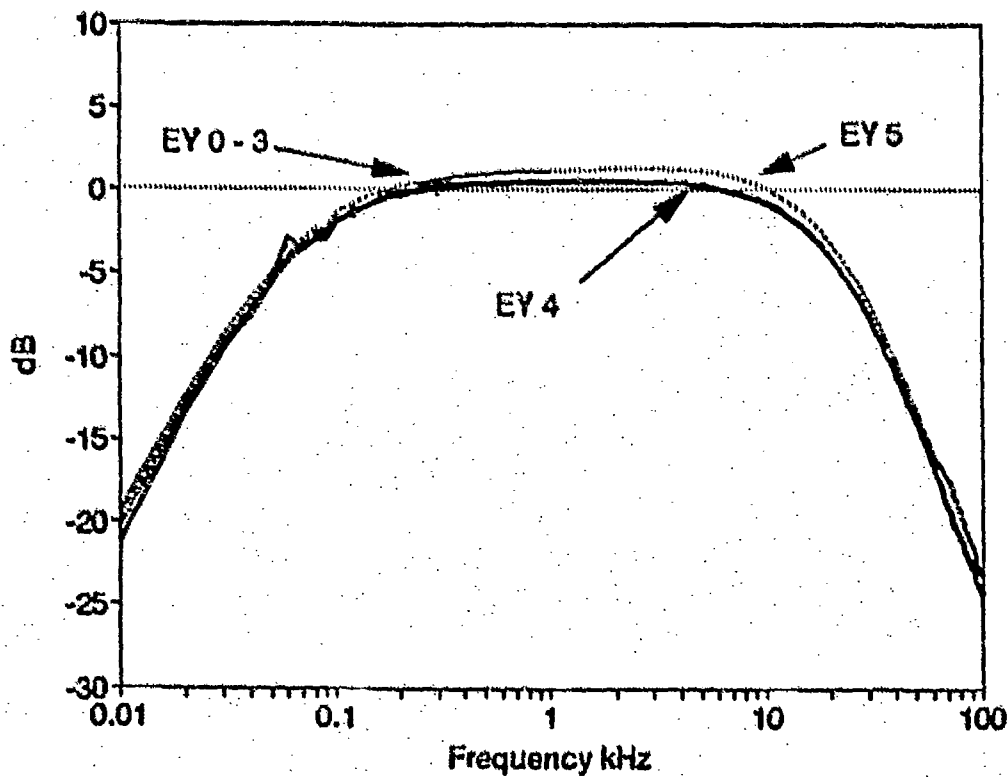
Element 2

Element 3

Element 4

C-3

EY 0, 1, and 2

EY 3

EY 4 and 5

EY 3 and 4 Data corrected for dB shift

Frequency kHz

Element 5

EY 4

EY 0, 1, 2, and 3

EY 3

EY 5

Ey 3, 4, and 5 Data corrected for dB shift

Frequency kHz
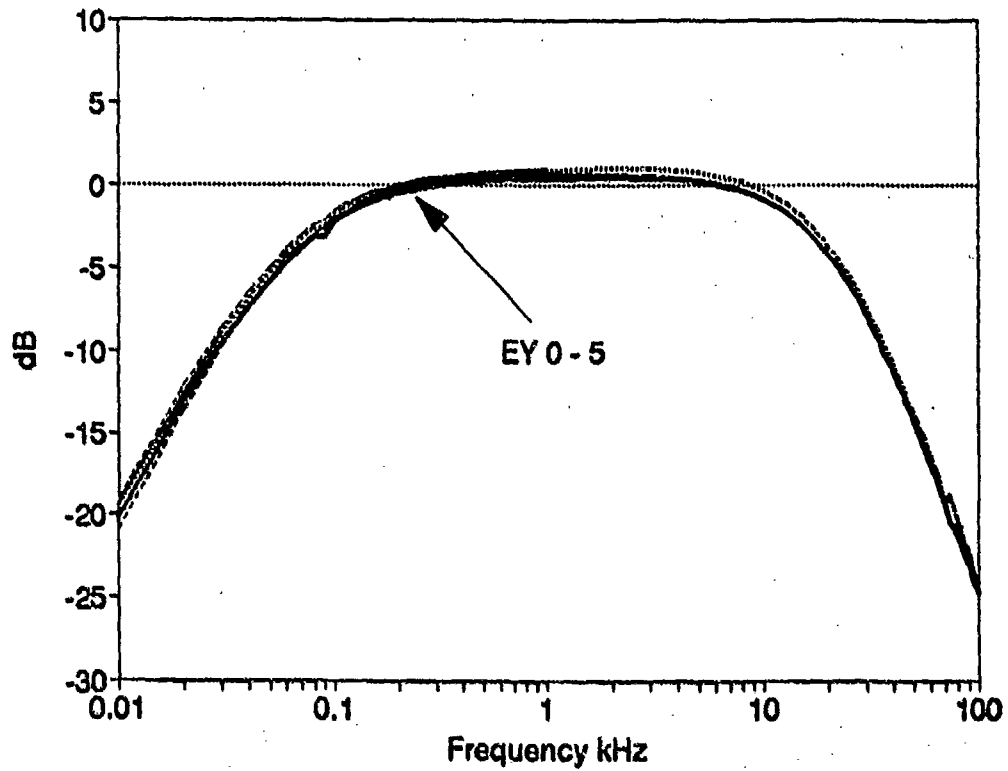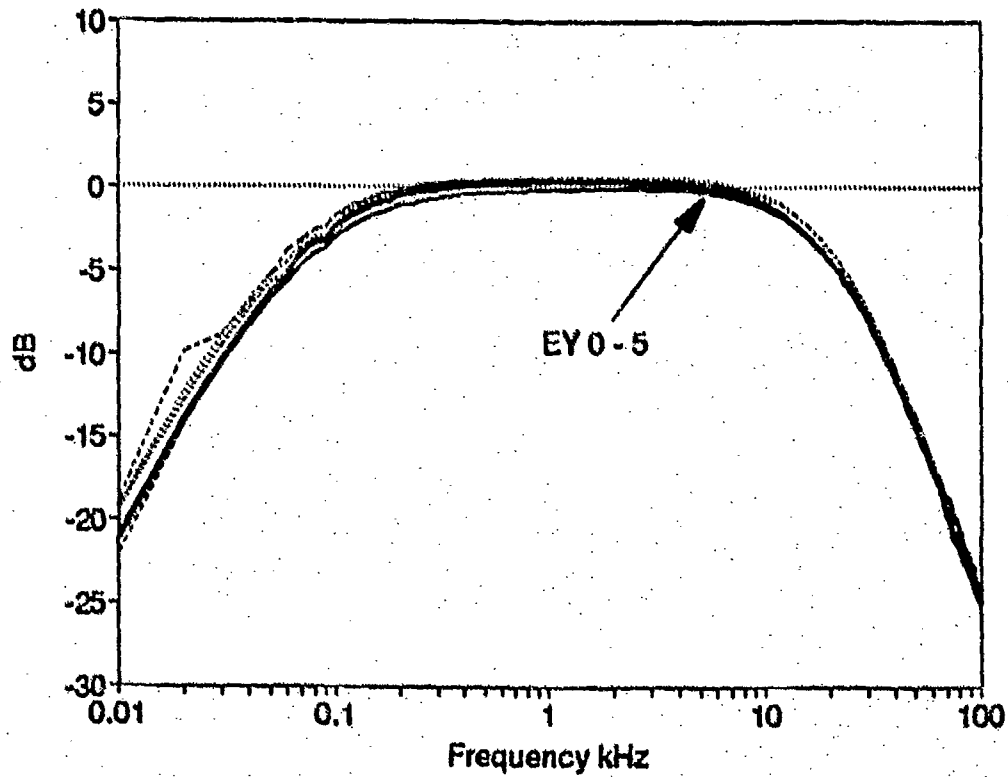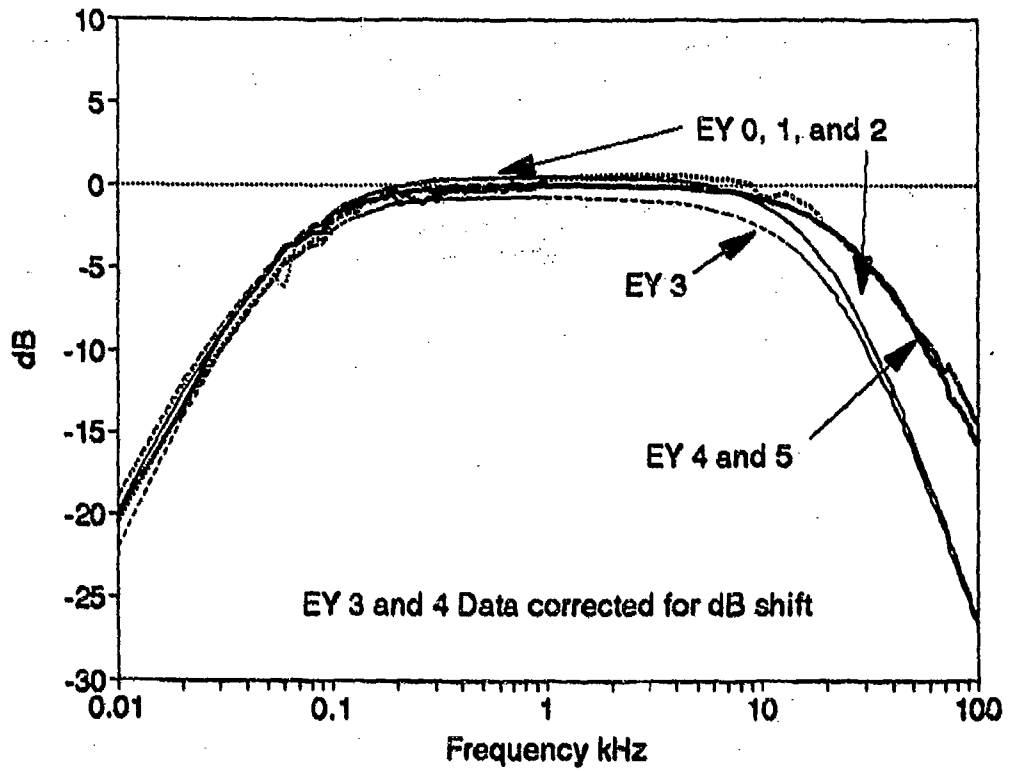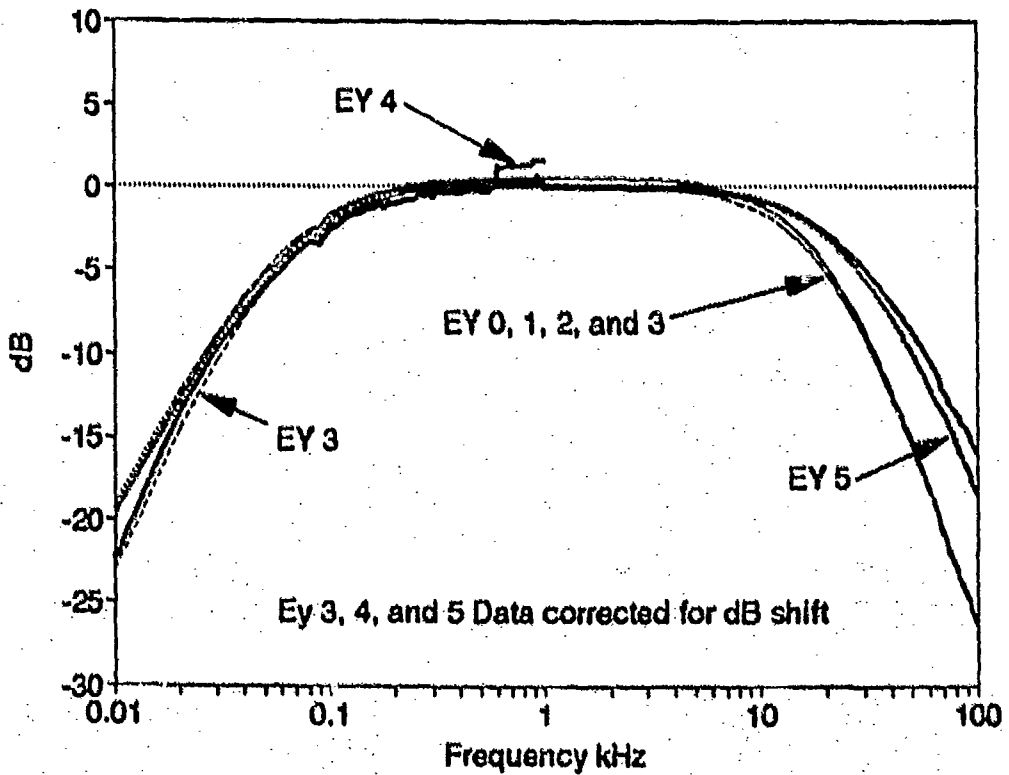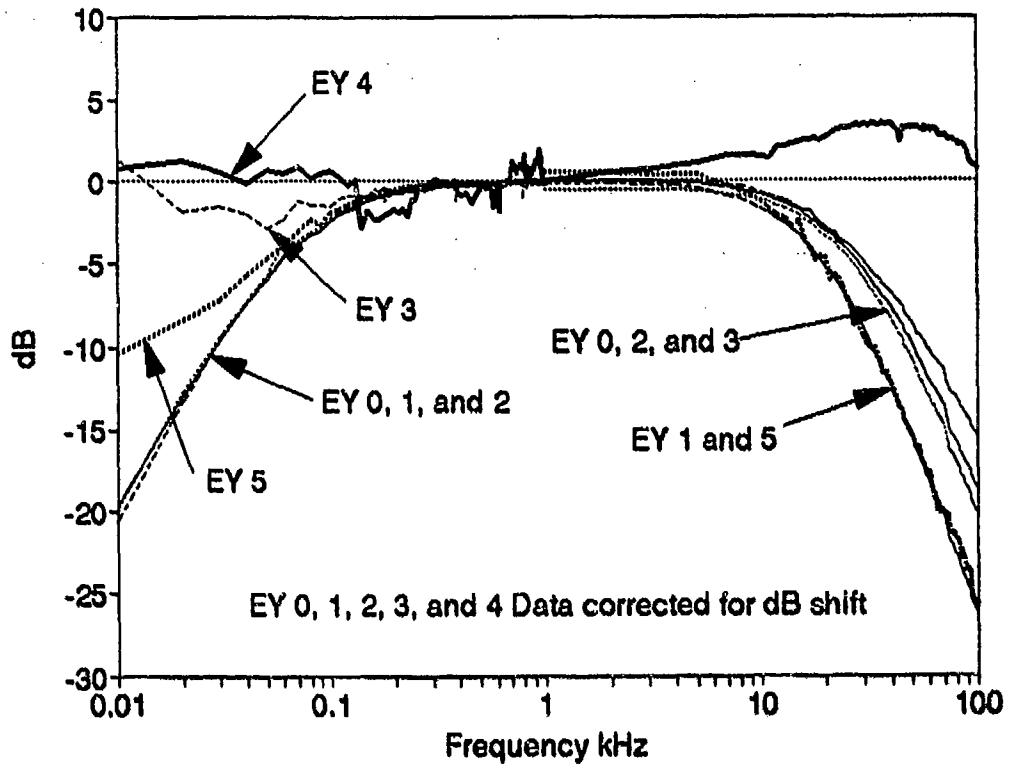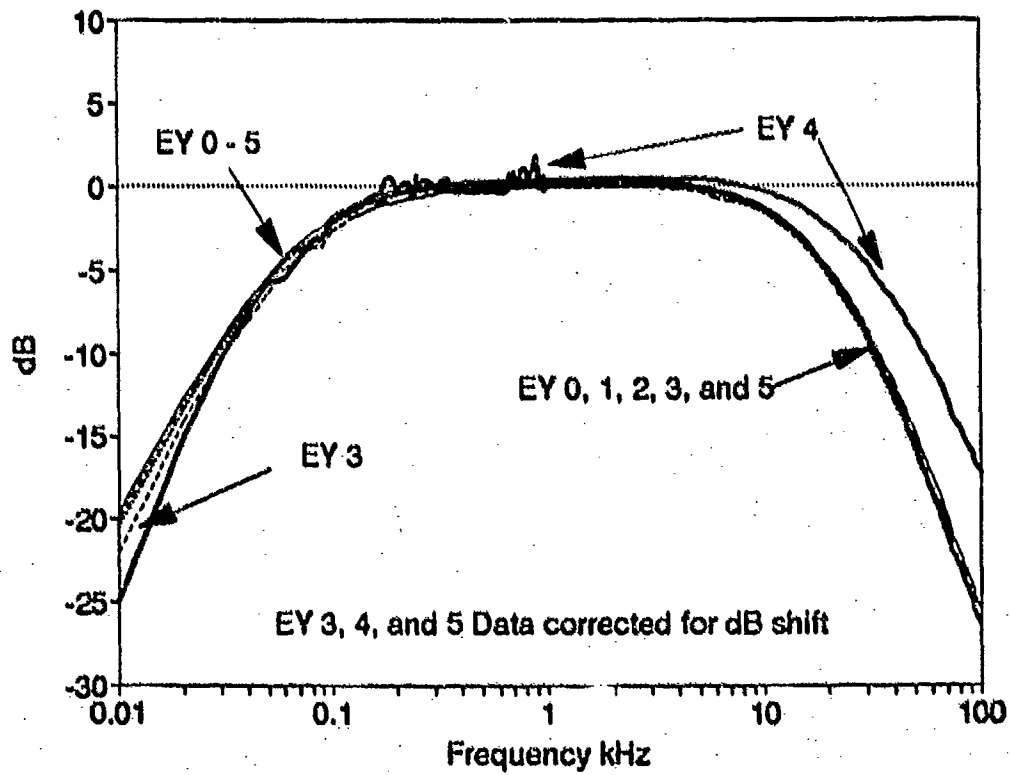
Element 6

Element 7

Element 8
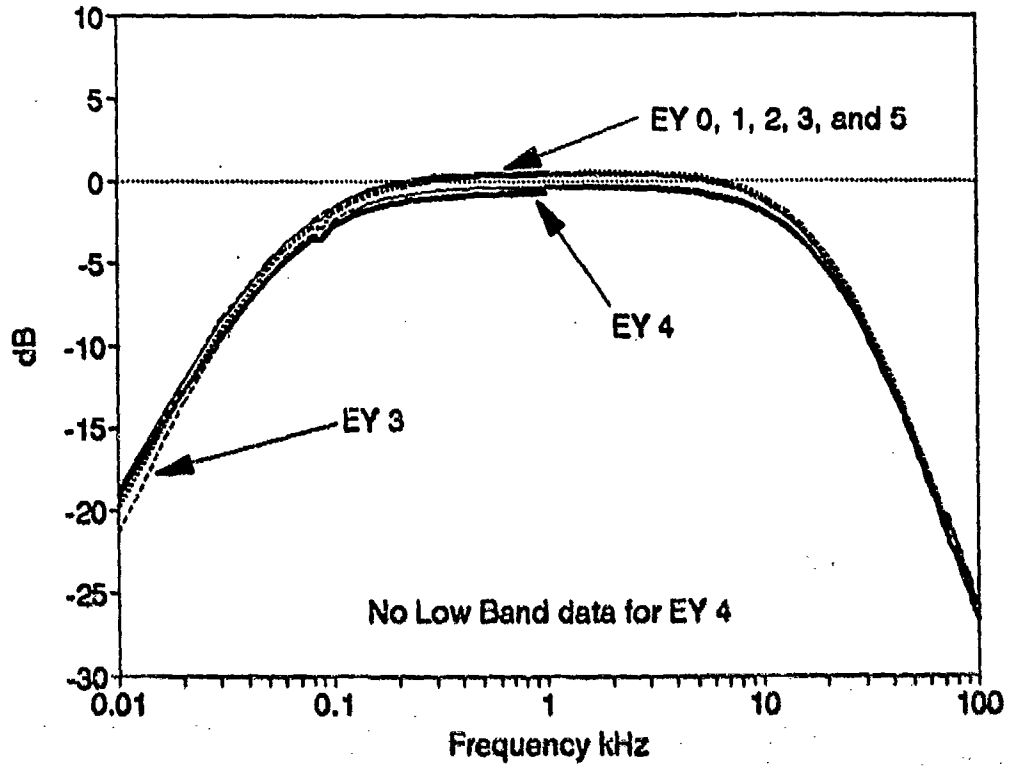
Element 9
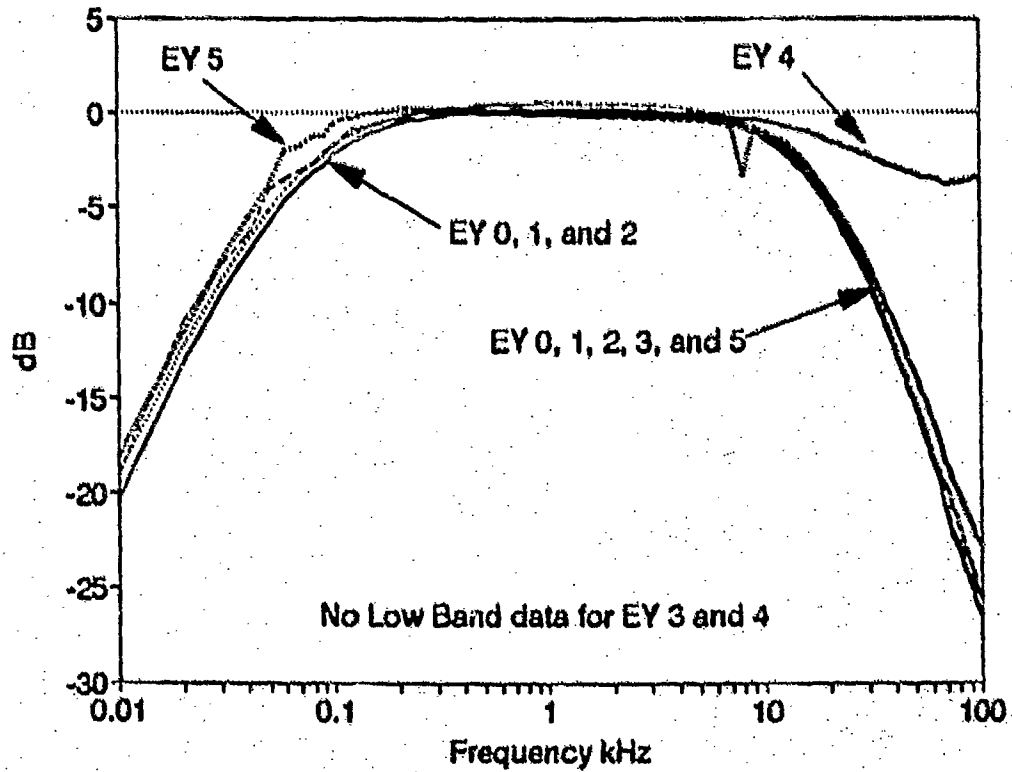
Element 10
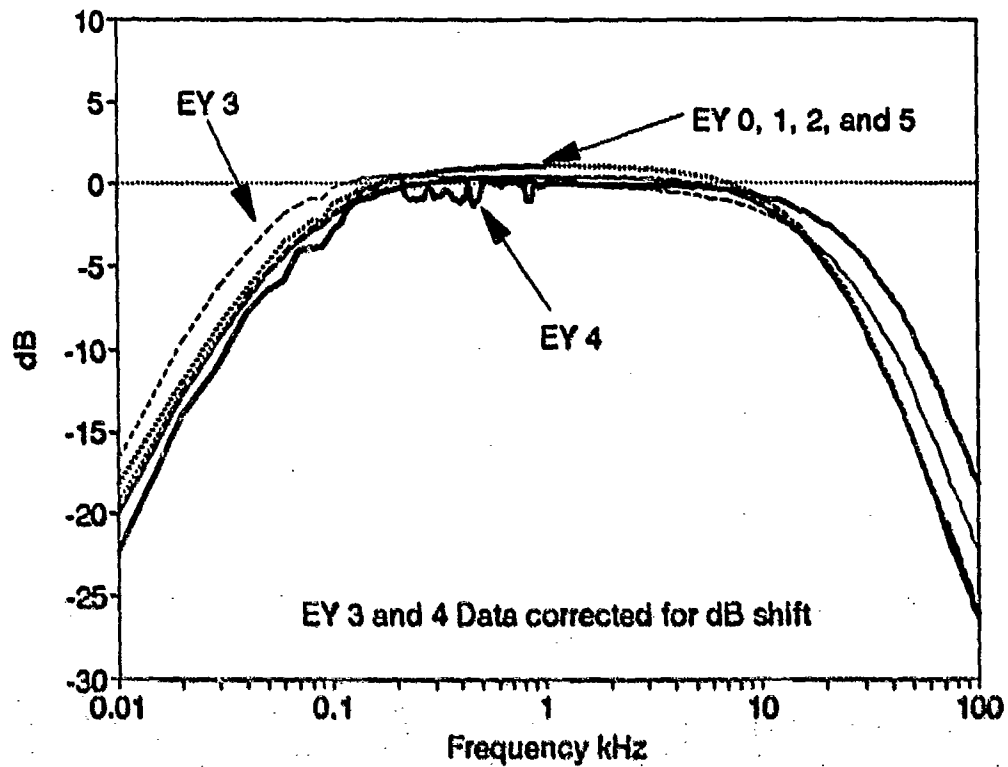
Element 11
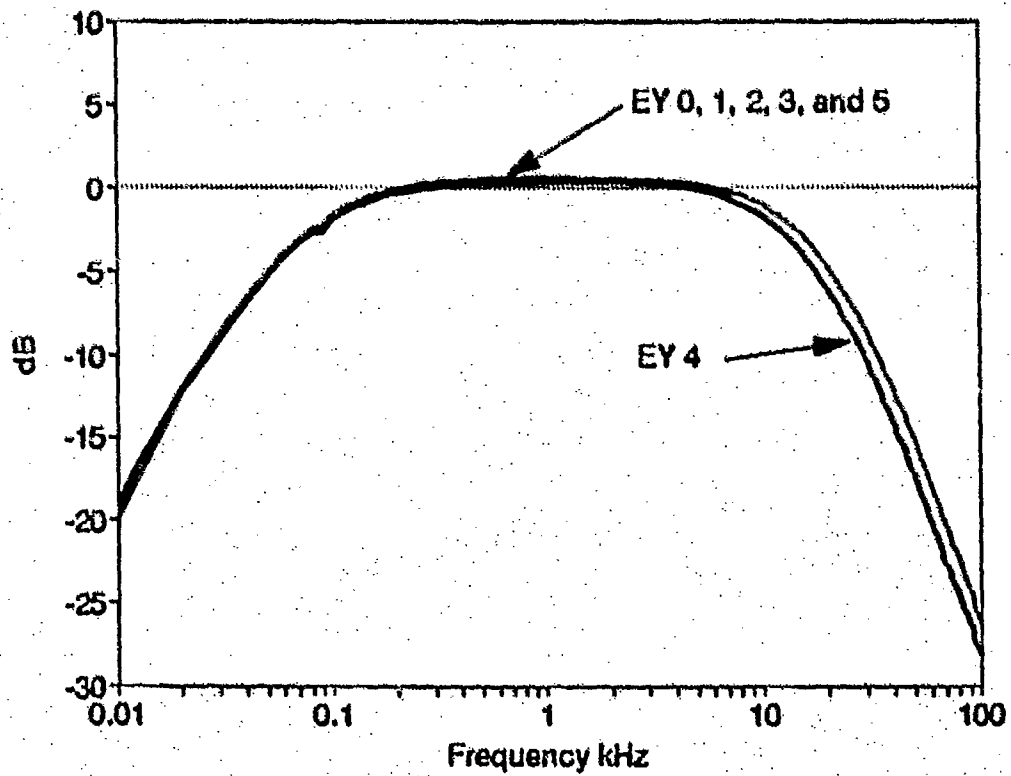
Element 12
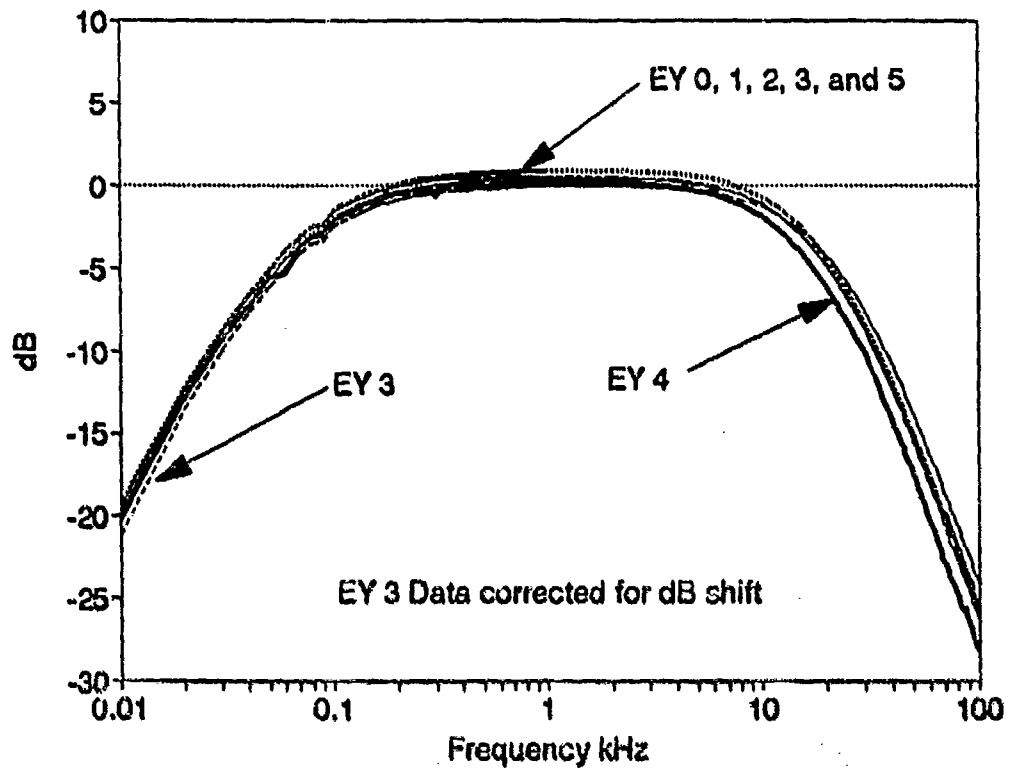
Element 13
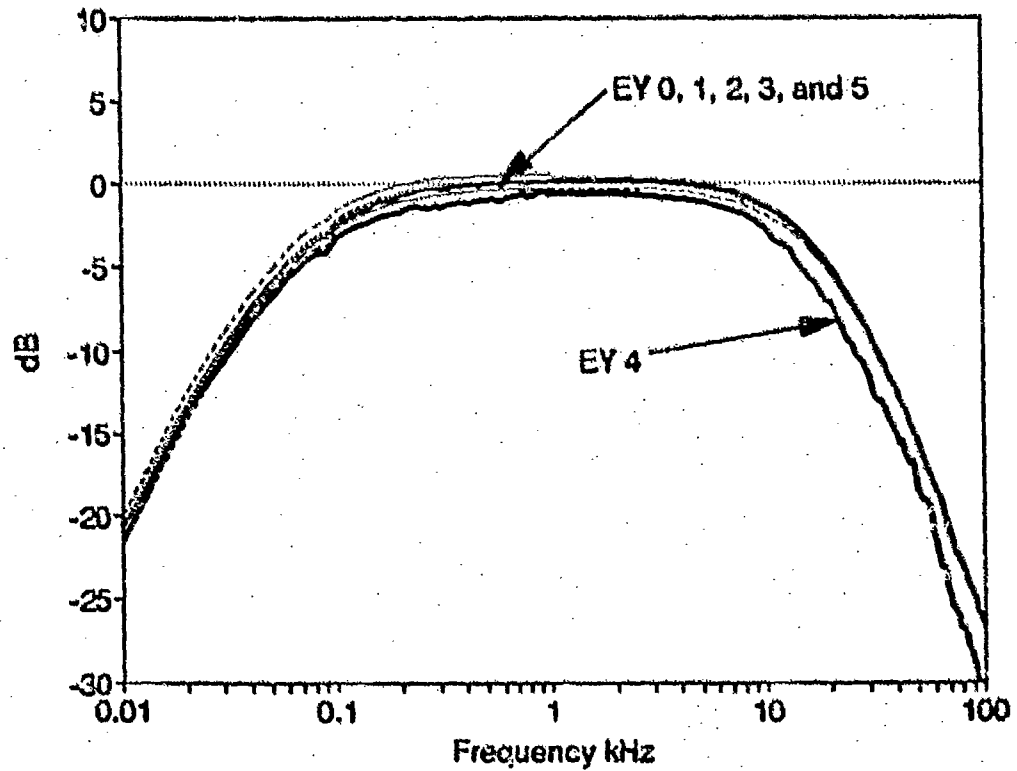
Element 14
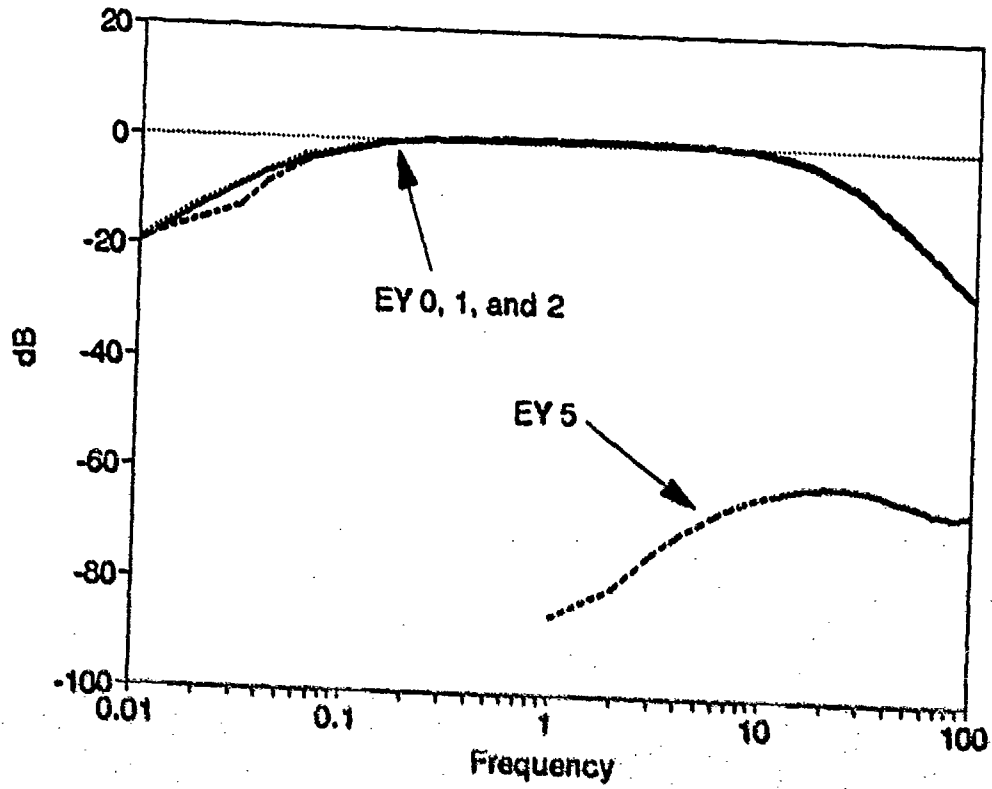
Element 15

Element 16

Element 17

EY 1 - 5 Data corrected for dB shift

Element 18

C-10
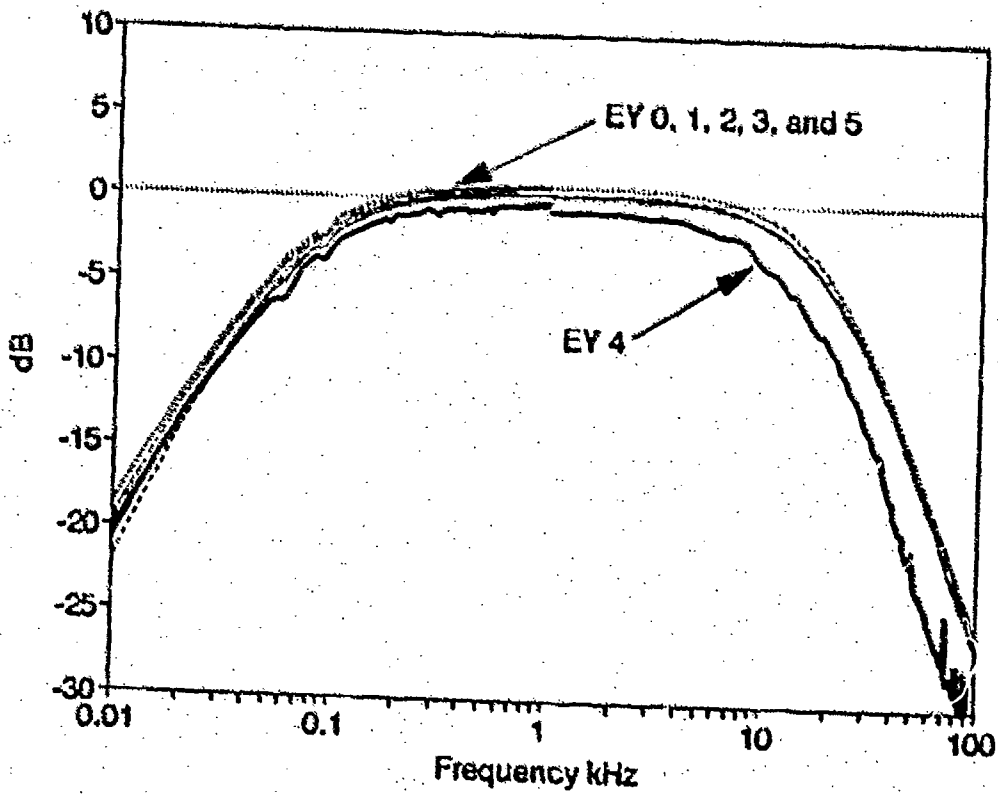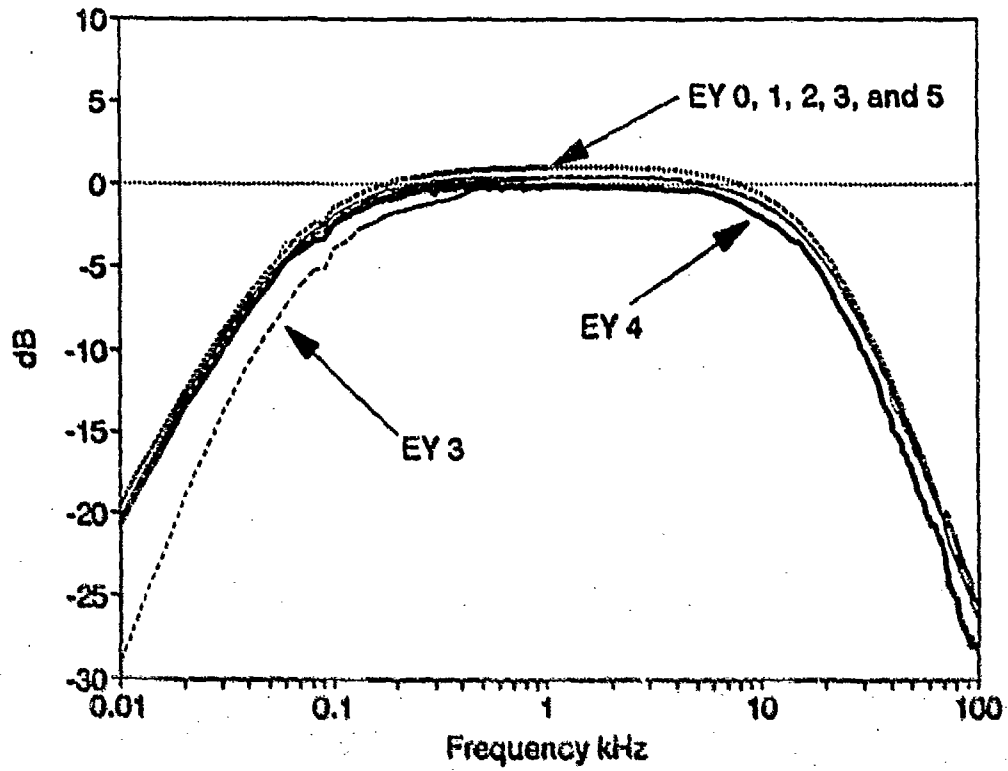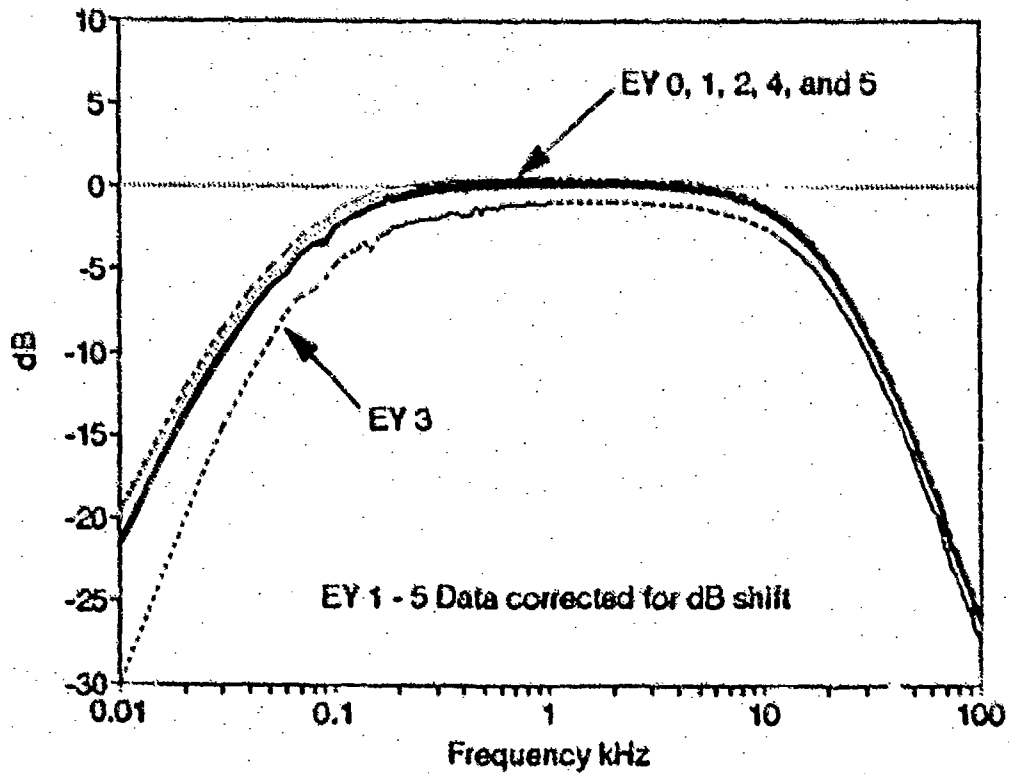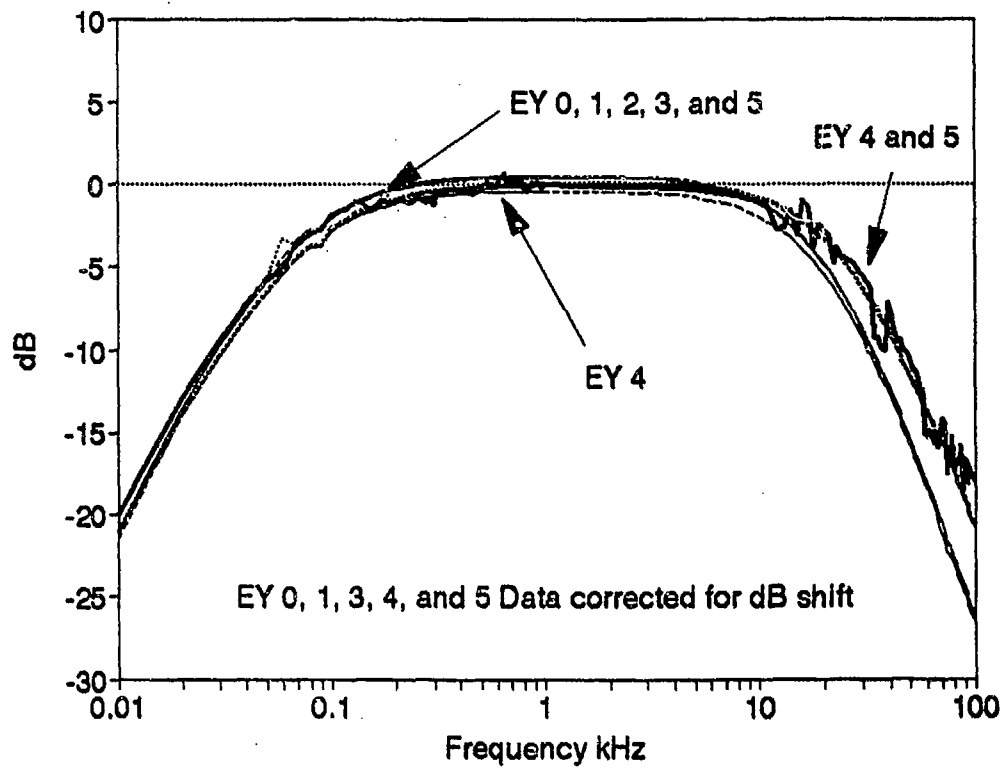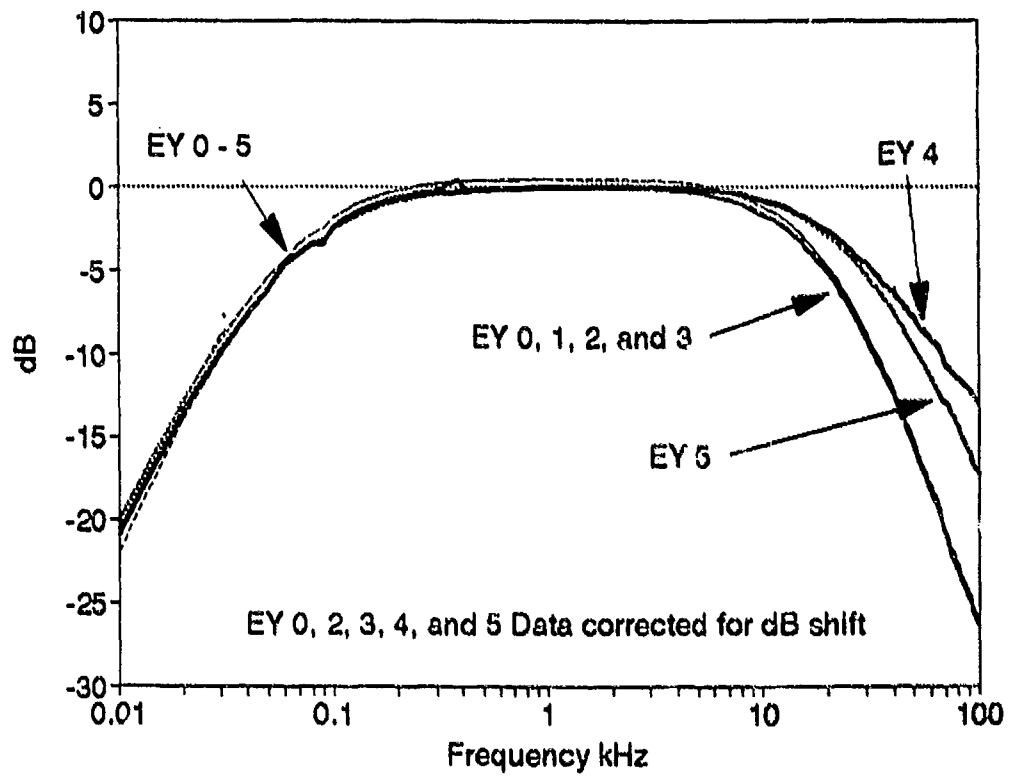
Element 19

Element 20

APPENDIX D

PHOTOGRAPHS OF HGA STAVE AUTOPSY
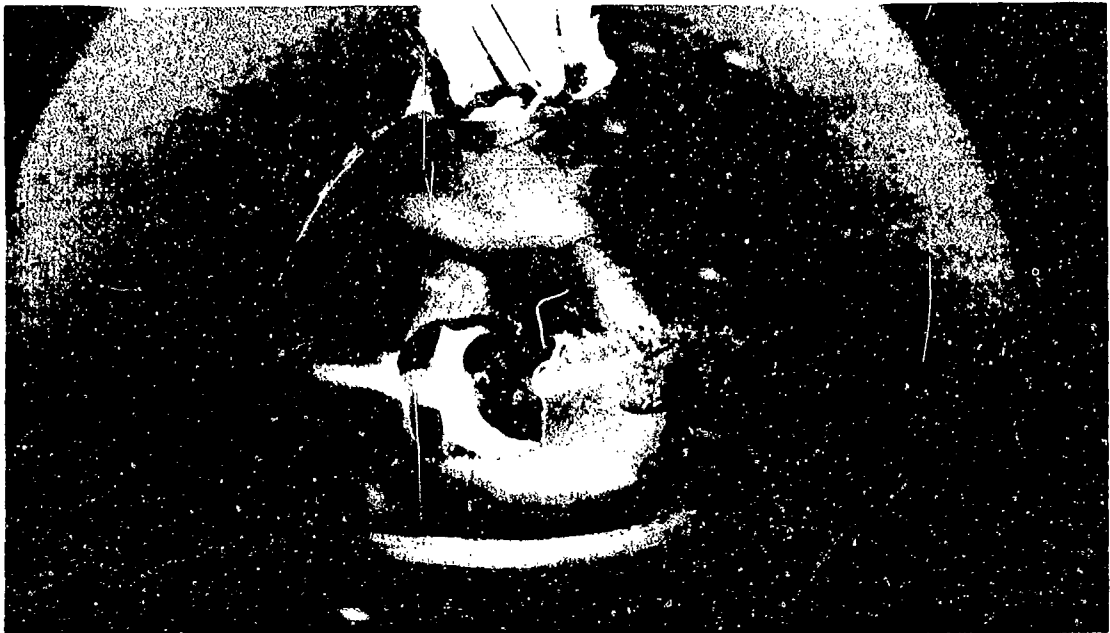
No. 1 – WATER DROPLET ON CONDUCTOR WITHIN MOLDING OF UNIT H7
(Repair site in molding made a convenient transparent window)
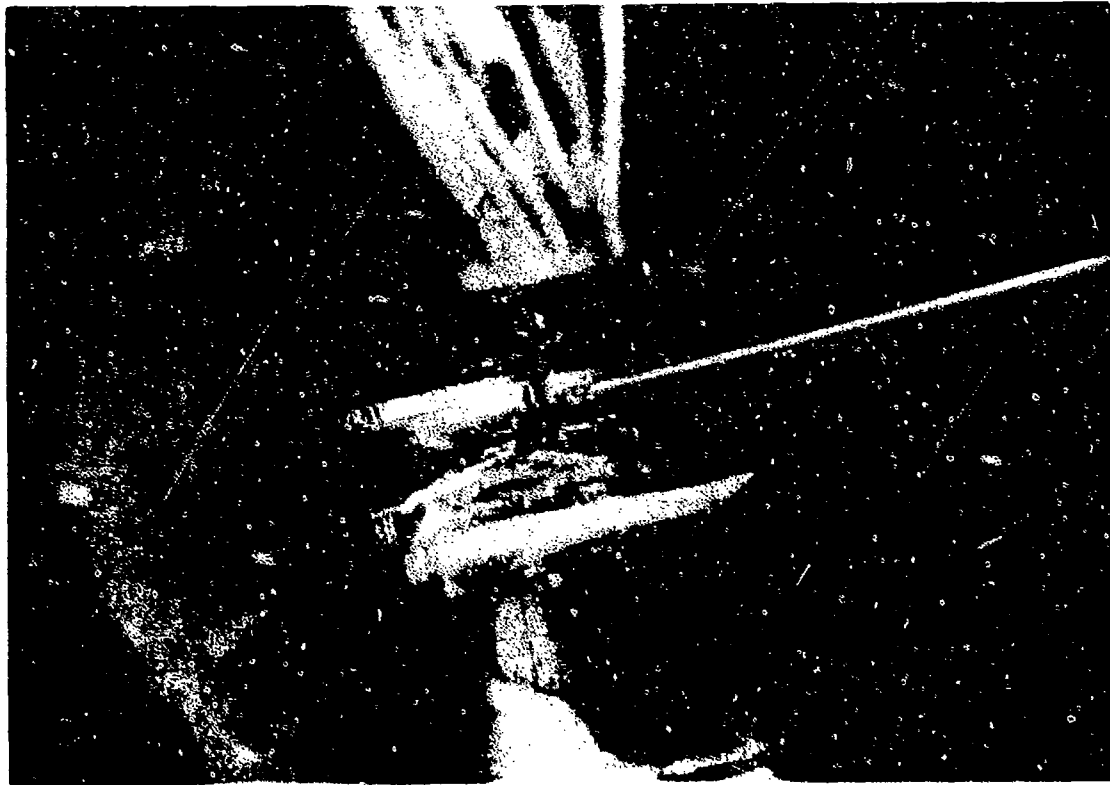
No. 2 – NEEDLE INSERTED AND IN CONTACT WITH WATER DROPLET
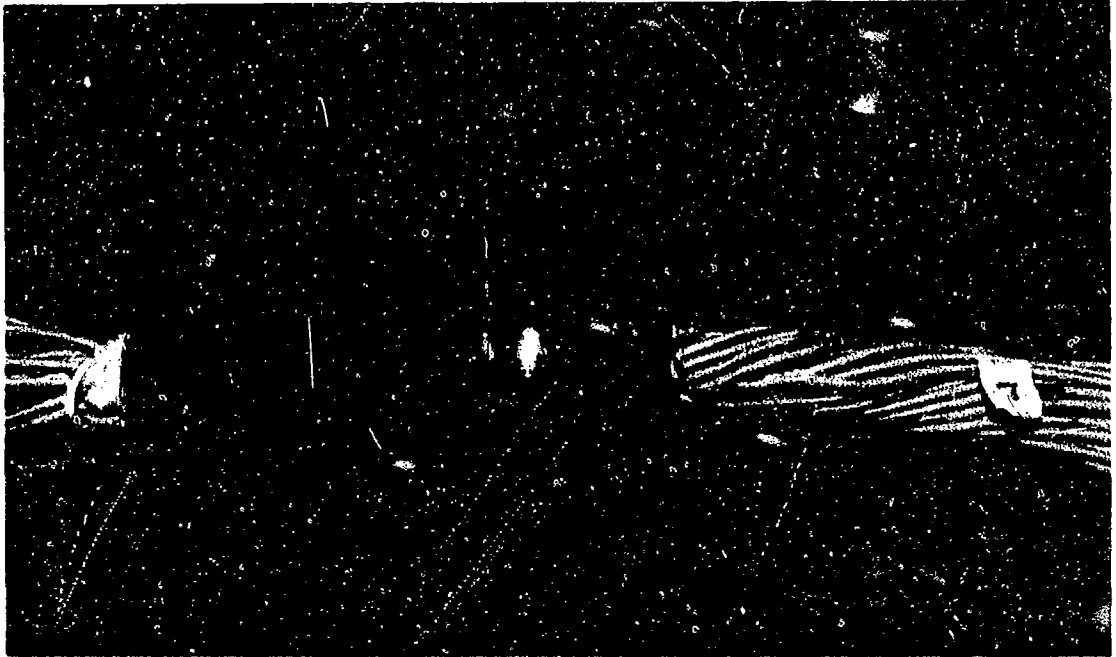
No. 3 – CONDUCTOR #7 KINKED AT ENTRY SITE INTO MOLDING
(conductor re-routed from normal lay for preferred entry site)

No. 4 – FLAWED PCB PRE-POTTED MOLDING ASSEMBLY (untinted)
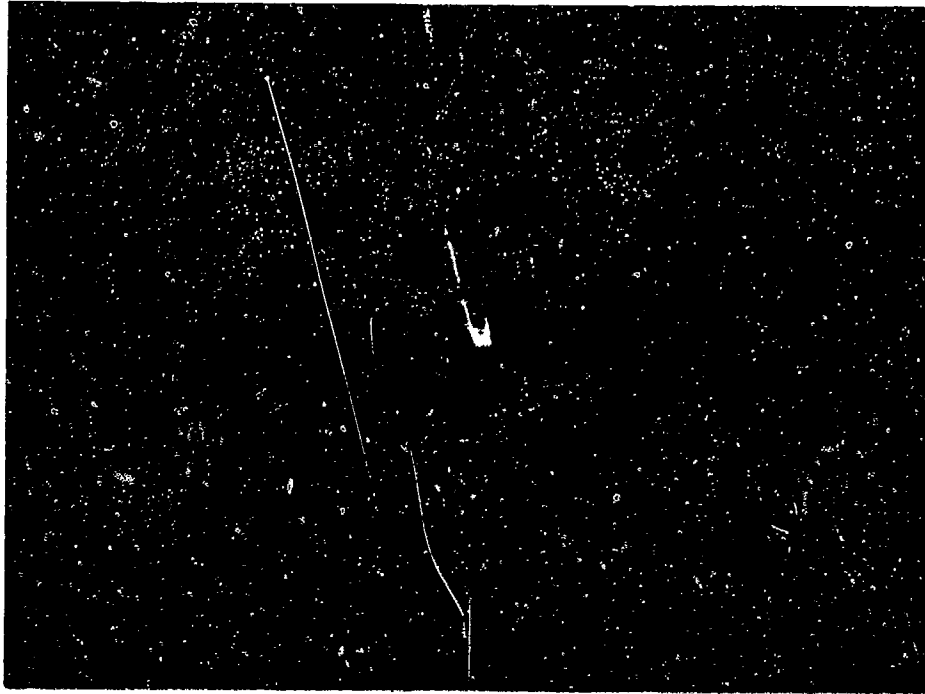
No. 5 – EXPOSED CAPACITOR LEAD BONDED TO SPOOL WITH EPOXY
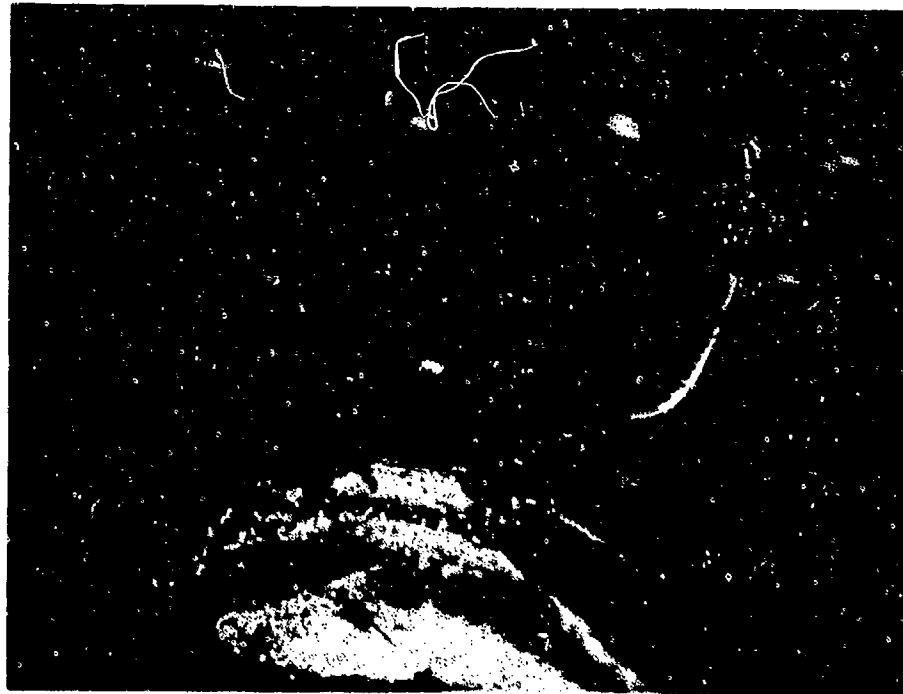
No. 6 – LEAD REMOVED FROM SPOOL
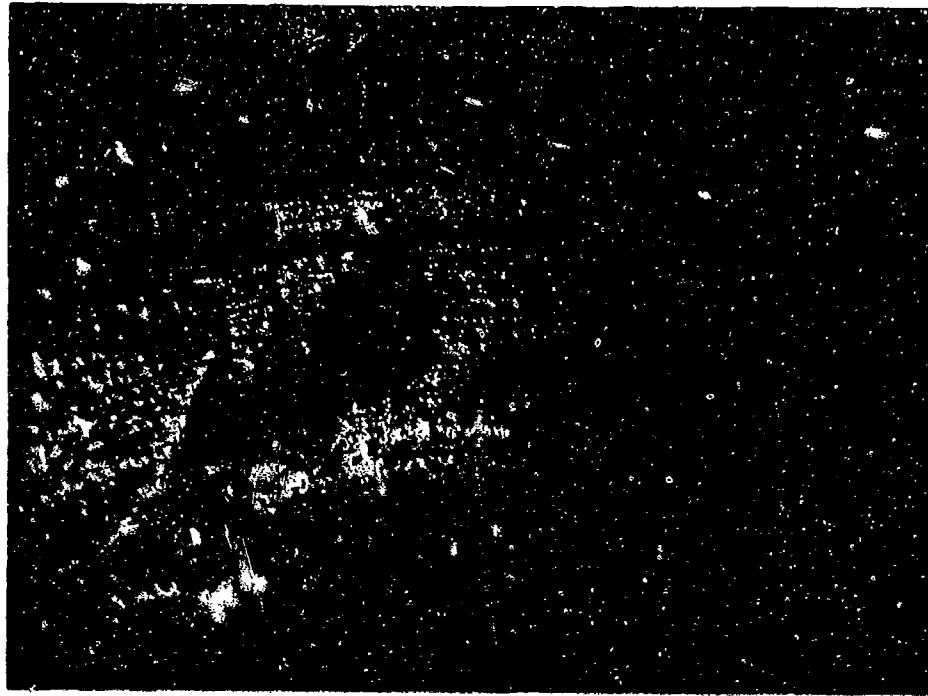
No. 7 – EPOXY VISIBLE WITHIN DRILLED HOLE IN SPOOL
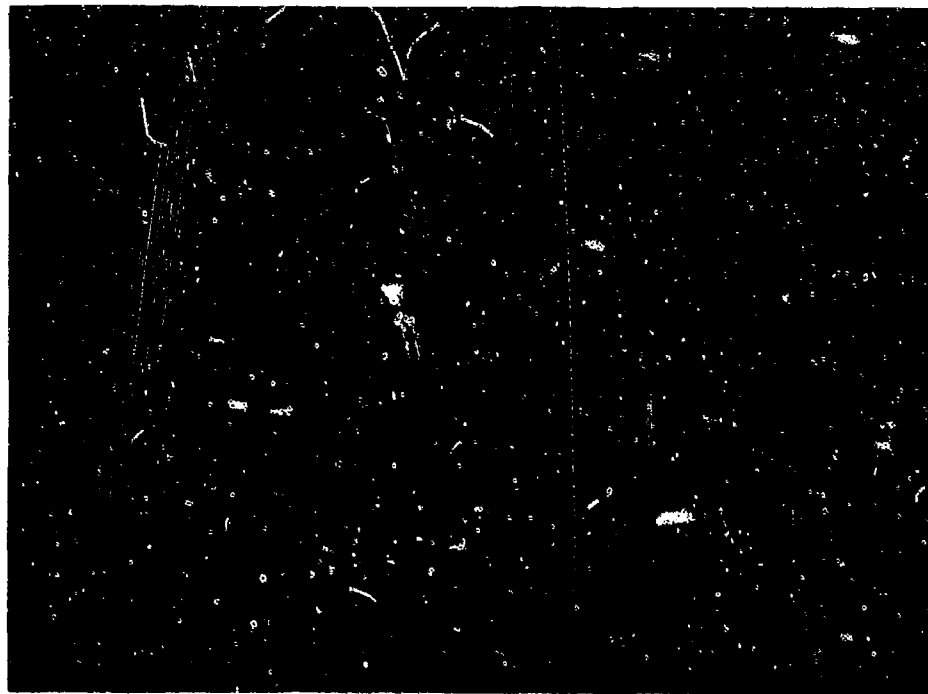
No. 8 – ROUGH SECTIONING OF SPOOL AND DRILLED HOLE